THESIS FOR THE DEGREE OF DOCTOR OF PHILOSOPHY

Experimental and modelling studies of particle radiation in flames

DANIEL BÄCKSTRÖM

Department of Energy and Environment

CHALMERS UNIVERSITY OF TECHNOLOGY

Gothenburg, Sweden 2015

Experimental and modelling studies of particle radiation in flames

Daniel Bäckström
ISBN 978-91-7597-183-4

Doktorsavhandling vid Chalmers Tekniska Högskola
Ny serie nr 3864
ISSN 0346-718X

Department of Energy and Environment
Chalmers University of Technology
SE-412 96 Gothenburg
Sweden
Telephone + 46 (0)31-772 1000

Reproservice
Gothenburg, Sweden 2015

Experimental and modelling studies of particle radiation in flames

DANIEL BÄCKSTRÖM
Division of Energy Technology
Department of Energy and Environment
Chalmers University of Technology

Abstract

Combustion of solid fuels is an important part of many industrial and power generation processes. The global use of coal in these processes is vast and thus also the related emissions of CO_2 to the atmosphere. It is not possible to continue on the path with continuously increasing emissions of CO_2 if the global climate targets should be met. Two strategies to reduce the emissions from large scale coal combustion is to apply oxy-fuel combustion, which is one of the proposed Carbon Capture and Storage (CCS) technologies, or to switch fuel from coal to biomass. Solid fuels are often combusted in pulverized form in flames, where radiation is the most important heat transfer mechanism. When firing solid fuels particle radiation is the dominating contributor to the radiative heat transfer. Application of either oxy-fuel combustion or fuel-switching in combustion processes will change the radiative conditions in the combustion chamber, which implies that knowledge about the main heat transfer mechanism is needed when designing or retrofitting furnaces for the new conditions.

The aim with this work is to develop a methodology combining measurements and modelling to quantify the radiative heat transfer in flames, with a special emphasis on the particle radiation features. Parameters, which are of particular importance in flame combustion such as particle temperature, particle type and size distribution have been measured, and the influence on the flame radiation has been analyzed using a detailed radiation model. The experimental work was performed in Chalmers 100 kW_{fuel} oxy-fuel test unit and in a 400 kW_{fuel} scale model of a rotary kiln furnace. In the 400 kW unit the influence on flame radiation of co-firing of coal and biomass was studied. The radiative intensity, measured with a narrow angle radiometer, has been used as reference data in all studies. An optical FTIR based system for measurement of the in-flame spectral radiation was tested and a system for extraction of particles from the flames was developed in this work. The particle size distribution and particle type were investigated using a low-pressure impactor and a scanning mobility particle sizer (SMPS). Detailed models describing the gas and particle properties were applied in the modelling work: a statistical narrow band model for the gas properties and Mie- or Rayleigh theory for the particle properties. In all investigated solid fuel flames, particles were found to dominate the radiation. In the investigated lignite flame in the Chalmers unit, char particles were found to be the main contributor with only a small influence of soot. In an analysis of spectrally resolved particle radiation, the temperature of the char particles was estimated to be approximately 200°C lower than the gas temperature in a position corresponding to peak temperature conditions of the flame. The soot volume fraction in a sooting air fired propane flame was determined to be 6E-8 based on measurements with the SMPS instrument, and this concentration resulted in a good agreement between modelled and measured intensity. The results from the 400 kW study showed that it is possible to obtain similar radiation intensity in the co-firing flames as in the coal flames. But, the length of the radiating part of the flames was shorter for the co-firing flames. Radiation measurements in flames of two almost identical coal types for similar combustion conditions revealed a significant difference in the radiative intensity. This result shows the difficulty of predicting flame radiation without performing measurements, since the radiation depends on factors such as soot formation, which is highly dependent on fuel and combustion conditions.

Keywords: *Radiative heat transfer, particle radiation, flame, coal, soot,*

List of Publications

This thesis is based on the following papers:

I. D. Bäckström, R. Johansson, K. Andersson, F. Johnsson, S. Clausen, A. Fateev, *Measurement and modelling of particle radiation in coal flames*, Energy and Fuels, 2014, 28 (3) pp 2199-2210.

II. D. Bäckström, D. Gall, M. Pushp, R. Johansson, K. Andersson, J. B. C Pettersson, *Particle composition and size distribution in coal flames – the influence on radiative heat transfer*, Experimental and Thermal Fluid Science, 2015, 64 pp 70-80

III. D. Bäckström, A. Gunnarsson, D. Gall, X. Pei, R. Johansson, K. Andersson, R. K. Pathak, J. B. C Pettersson *In-flame measurements of the volume fraction and optical properties of soot in an 80 kW propane flame*, to be submitted for publication

IV. D. Bäckström, R. Johansson, K. Andersson, F. Johnsson, S. Clausen, A. Fateev, *Gas temperature and radiative heat transfer in oxy-fuel flames,* Clearwater Clean Coal Conference, 2012

V. D. Bäckström, R. Johansson, K. Andersson, H. Wiinikka, C. Fredriksson, *On the use of alternative fuels in rotary kiln burners – an experimental and modelling study of the effect on the radiative heat transfer conditions*, submitted for publication.

Daniel Bäckström is the main author of paper I - V and responsible for the experimental work and evaluation of the data. Dr. Robert Johansson has contributed with guidance in the modelling and together with Professor Klas Andersson and Professor Filip Johnsson with discussions and the editing of the papers.

Acknowledgements

I would like to express my gratitude to my main supervisor Klas Andersson for your wholehearted support and constructive inputs throughout this work. Your positive attitude is highly appreciated and has made my work easier. Thank you Robert Johansson for always taking the time for discussing my work, for transforming my drafts into readable text and for all the help with the radiation modelling. Filip Johnsson is acknowledged for introducing me to this interesting field of research and for the editing of the texts.

During the experimental work I have received invaluable help from a number of persons: Thomas Ekvall, Daniel Fleig, Johannes Öhlin, Dan Gall, Rustan Marberg, Ulf Stenman, Jessica Bohwalli, Adrian Gunnarsson, and Daniel Kühnemuth. Your help is gratefully acknowledged! I would specially like to thank Thomas Ekvall, it has been great working with you during these years. To all others at the Division of Energy technology who I have not mentioned, thank you for creating a nice work environment. Henrik Jilvero, I do enjoy the extra space in the office after you left. But, it was more fun sharing office with you.

I would also like to thank the co-authors of my articles. Your input to this work is very much appreciated.

LKAB and the Swedish Energy Agency are gratefully acknowledged for financial support. I would especially like to thank Christian Fredriksson, Bosse Lindblom and Johan Sandberg at LKAB for a good co-operation.

Finally, I would like to thank my family and friends for being there for me. To my beloved Kristin, thank you for your endless support throughout these years. I love you and I look forward to our future together. Lastly, to Tyra, despite keeping me awake at night your smile in the mornings provides me with energy which lasts all day.

March, 2015

Daniel Bäckström

Table of content

Outline

This thesis consists of a summary of the work and five appended papers (Paper I-V). First, a short background to the work focused on the interrelation between the radiative heat transfer and different combustion processes is given. Previous work in the field is discussed, important areas are highlighted and the aim and scope of the work is defined. The following chapter gives a theoretical background to radiative heat transfer and introduces important concepts. A review of measurement techniques relevant for studies of flame radiation is presented in Chapter 3. In Chapter 4 the experimental facilities used and investigated test cases used are described, and Chapter 5, presents the applied radiation models including both particle and gas radiation. A summary of the results from Papers I - V are summarized in Chapter 6, while the two final chapters include conclusions and ideas for future work.

Paper I presents a methodology where in-flame measurements and detailed modelling are combined to directly quantify particle radiation in a lignite flame. A method for estimation of the maximum amount of soot in the flame is also presented. Paper II is based on extractive particle measurements from the high temperature zone of a lignite flame using a low-pressure impactor. The work is focused on the influence on radiative heat transfer from different particle types and sizes using detailed models for the evaluation of the gas and particle radiation. In Paper III, soot in an air fired propane flame was studied with the aim of characterizing the particle radiation under well-defined conditions. The volume fraction and optical properties of soot was measured and the influence on the particle radiation was shown. Paper IV includes an evaluation of the FTIR-based measurement system for gas temperature measurements in a 100 kW flame, which is the scale of the flame in Chalmers oxy-fuel rig. Based on the measured temperature fluctuations, a simplified approach is applied to estimate the influence of Turbulence-Radiation Interactions in the flame. Paper V is a study of different fuels used in a pilot scale model of a rotary kiln furnace. The radiation intensity for a number of fuels and fuel mixes are studied with the aim of evaluating if they are suitable for large scale implementation in a grate-kiln process used for iron ore production.

1. Introduction

Energy conversion by combustion of solid fuels, mainly coal, is one of the main processes used for power generation today. The use of coal is also essential in a number of industrial processes, for example cement, iron ore and steel production. However, the use of coal and other fossil fuels is problematic due to the associated emissions of CO_2 and the related effect on global warming. Although efforts are made to decrease the use of coal in the electricity generation sector as well as in industrial applications, the global use of coal continues to increase [1], and, to fulfil the climate targets suggested by *e.g.* the IPCC remains as a tremendous challenge for society. Carbon Capture and Storage (CCS) technologies, such as oxy-fuel combustion [2], has been proposed as one of the main options for continued use of fossil fuels in the electricity production system, while avoiding emissions of CO_2 to the atmosphere. Another option to avoid net emissions of CO_2 is to switch to carbon neutral fuels such as biomass. Both oxy-fuel combustion and a switch of fuel imply major changes of the combustion conditions in the process. In combustion chambers, radiative heat transfer is the dominating heat transfer mechanism, and typically transfers 90% of the total heat. In combustion systems, where solid fuels are burned, particle radiation constitutes a large part of the radiative heat transfer. A fundamental understanding of the radiative heat transfer mechanism is therefore important when designing new furnaces, but also for optimization of existing furnaces. Large scale implementation of oxy-fuel combustion requires a better knowledge of the heat transfer mechanisms in the combustion chamber since the conditions in terms of temperature and gas concentrations in the furnace can be fundamentally different. The radiative heat transfer conditions are also highly dependent on the fuel used with effects on the particle size distribution and concentration as well as temperature conditions. To be able to predict the influence from these types of changes on the heat transfer conditions requires a thorough understanding of the relevant radiative heat transfer mechanisms. This work is devoted to radiative heat transfer in flames with special emphasis on oxy-fuel combustion and combustion in rotary kilns and the work is based on a combined experimental and modelling approach.

1.1 Studied applications

Large scale generation of electricity in combustion processes is normally done in two types of boilers; pulverized coal fired boilers (PC) or in circulating fluidized bed boilers (CFB). These plants are often very large with a thermal input in the order of several hundred MW_{fuel}. Modern large power plants often have supercritical or ultra-supercritical steam data, *i.e.* pressure and temperature above the critical point of water. In PC boilers coal is used in pulverized form in which the coal is milled to a size of 5 – 400 μm and combusted in a number of diffusion flames in the combustion chamber [3]. Heat from the flames is transferred, mainly by radiation, to the water walls where the steam is produced. Depending on the fuel, different particles are present in the different zones of the furnace. In the flames fuel, soot and ash particles co-exist; further downstream the ash and unburnt char particles dominate. As indicated above, radiation dominates the heat transfer in the furnace and in the flames the particles are the main contributor to the radiation, while the conditions further downstream are characterized by lower temperature and less particle radiation and consequently the gas radiation becomes more important. In fluidized bed boilers the temperature is generally lower due to the high concentration of inert solid material, and the radiative heat transfer is thus of less importance. In oxy-fuel combustion of coal, the air supplied to the burners is replaced by recirculated flue gases mixed with pure oxygen, Fig 1.1. This results in an atmosphere in the combustion chamber dominated by absorbing and emitting gases, mainly CO_2 and H_2O, instead of N_2 which is transparent to radiation. This changes the gas radiation conditions in the furnace. The higher heat capacity of CO_2 compared to N_2 also leads to a lower gas and flame temperatures in oxy-fuel combustion. Wall et al. [4] recognized that furnace design is often based on previous experience and that the changed radiation conditions in the furnace may cause problems when retrofitting existing air fired boilers to oxy-fuel combustion. Oxy-fuel combustion also provides more possibilities of adjusting the combustion conditions. By decreasing the amount of recirculated flue gas it is possible to adjust the flame temperatures and thereby to alter the heat transfer in the combustion chamber. If drastic changes are made, *i.e.* using significantly higher O_2 fractions in the oxidizer, it is possible to design more compact boilers due to the decreased volume flow [5]. However, such large modifications require a fundamental knowledge of how the heat transfer mechanisms, including particle radiation, are affected.

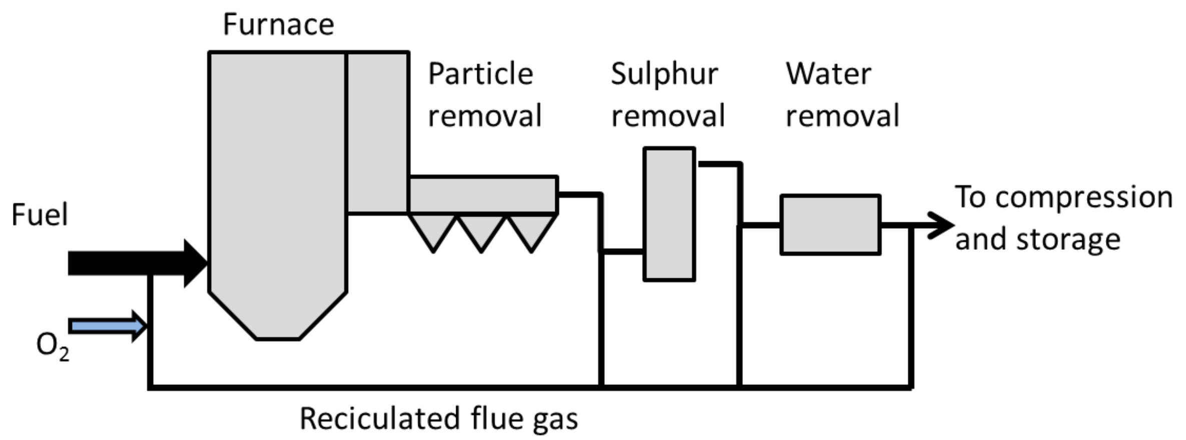

Figure 1.1. Schematic figure of the oxy-fuel process.

Iron ore is one of the most important mining products in the world. The ore from the underground mine is first treated in a process to separate the iron ore from the rock, it is then crushed, cleaned from impurities and mixed with additives. The product then enters a pelletization plant where the iron ore is sintered into hard pellets which can be transported. The grate-kiln process is often used for the sintering and oxidation of the pellets. A description of a typical plant can be seen in the work by Jonsson et al. [6]. The grate-kiln process consists of three parts, a travelling grate, a rotary kiln and a cooler. The pellets are dried, heated and partly oxidized on the travelling grate before it enters the rotary kiln. The final oxidation and sintering of the pellets take place in the rotary kiln. A very large air flow is supplied through the pellet bed in the cooler. A part of this pre-heated air is supplied to the rotary kiln, see Fig. 1.2. A burner is placed centrally in the back-end of the rotary kiln where coal or oil is normally burned and the flame stretches far into the kiln to obtain a homogeneous heating of the pellet bed by direct radiation from the flame and by radiation and conduction from the hot kiln wall. The temperature of the pellets leaving the rotary kiln is around 1200°C. A typical rotary kiln in these plants is 40 m long, approximately 6 m in diameter and is rotating with around 2 rpm. Due to the dimensions of the kiln and the fact that it is rotating makes radiation measurements inside the kiln very challenging. The temperatures in the kiln are in general higher than in the combustion chamber of a boiler used for electricity production due to the high pre-heating of the air and less cooling by water walls. The air is supplied via the pellet cooler (C1 in Figure 1.1) and enters the kiln with a temperature of about 1150°C. The air to fuel ratio is in the range of 5-6 in the combustion process and this is hence another important difference compared to the flame conditions in a power plant.

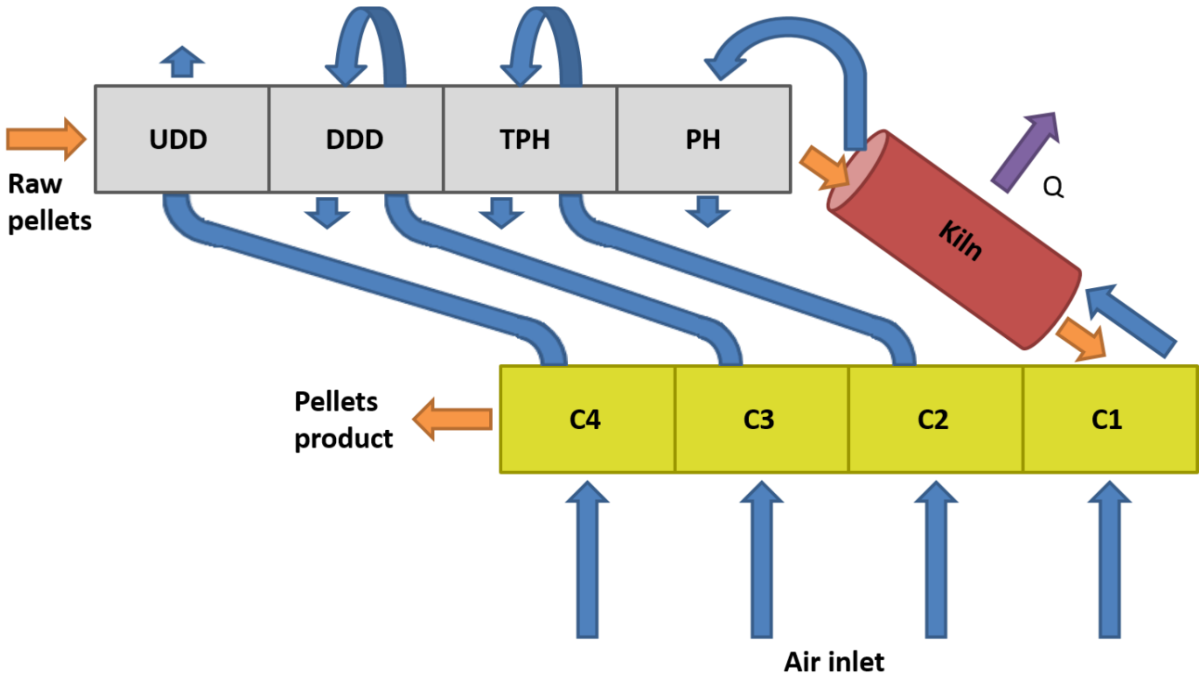

Figure 1.2. Schematic figure of the grate-kiln process of iron-ore production, travelling grate (UDD, DDD, TPH, PH), kiln and cooler (C1-C4).

1.2 Previous work

In a comprehensive review of radiative heat transfer in combustion applications Viskanta and Mengüc [7] stressed the importance of radiation and pointed to some specific areas of high interest for further investigations. One of the areas identified was particle radiation and the radiative properties of the various particles present in a combustion chamber. Experimental methods for model verification and the need of experiments in large scale burners and combustion devices were also discussed as important areas. Another review on flame radiation by Tien and Lee [8] concluded that detailed information about gases and soot is needed for accurate predictions of the flame radiation. Many of the studies are now more than

20 years old and the development of measurement techniques has progressed far since the reviews by *e.g.* Viskanta and Mengüc [7] and Tien and Lee [8]. Also, the computational power in modern computers have increased significantly so advanced models can now be used on a standard computer. More recently, the research on combustion of solid fuels has paid considerable attention to oxy-fuel combustion. In a review of the current state-of-the-art in oxy-fuel combustion [9] important topics in the development of the oxy-fuel combustion technology were discussed. Some of the topics highlighted were related to radiative heat transfer, *e.g.* the need for experimental data and the development of radiation models.

Despite the importance of radiative heat transfer in combustion, detailed studies of radiative heat transfer in flames of technical scale is scarce. Radiative heat transfer studies generally require a certain flame scale to produce results representative for industrial flame conditions due to the short pressure-path-lengths and low particle concentrations in small flames. However, small lab scale experiments, *e.g.* entrained flow reactors and small burners, are well suited for studying various combustion phenomena important for the radiative heat transfer [10-15]. Most measurement techniques are also developed and tested in small scale reactors before implementation in large scale experiments. For example two-colour pyrometry for particle temperature measurements was used early in small test rigs [12, 16], and is now used in larger facilities, as presented in *e.g.* Refs. [17-19]. Measurement of particle temperature with FTIR was demonstrated by Solomon et. al [14] in lab scale applications and has since then been used and refined by several groups [20-24].

The lack of comprehensive works on radiative heat transfer in flames of technical scale was recognized by Butler et al. [17] who studied the radiative heat transfer in a 100 kW coal flame. The same group has also presented several other relevant studies focused on coal combustion [19, 25-29]. The aim of the work of Butler and co-workers was to present a complete set of data to perform detailed analysis of the radiation from the flame using data previously unavailable in the literature. The flame was characterized using *e.g.* ellipsoidal element for radiative heat flux, two-color pyrometry for particle temperature measurements and suction pyrometry for measuring the gas temperature. The measured radiative heat flux was compared with calculated incident wall flux using a wide band model for the gas properties and a simplified expression for the absorption coefficient of soot. However, the soot volume fraction was not measured but instead estimated based on the volatile content of the fuel. Fletcher et al. [25] reviewed work on soot in coal combustion. The formation of soot from different coal ranks was discussed and one of the conclusions from the review was that there is a limited amount of data on soot formation available from actual combustors. The formation of agglomerated soot particles in the post flame zone was also discussed. Measurements of agglomerated soot particles in the size region 5 – 38 μm was presented, which means that the soot agglomerates start to scatter radiation. The results by Seeker et al. [30] shows that tar-rich coals are more likely to form soot, which means that bituminous coals tend to form more soot than sub-bituminous coals, lignite and anthracite. In a recent work Draper et al. [19] used two-colour pyrometry to obtain two-dimensional images of the particle temperature in an oxy-coal flame. One grey, and one spectral soot emissivity model was used to determine the particle temperature and emissivity. They analysed the images and discussed the way soot and char particles would appear in the images. Mie-theory based calculations were performed for spherical soot and char particles, 30 nm and 60 µm in diameter respectively, and it was concluded that soot is the dominating emitter. They concluded that the non-grey model was more accurate than the gray model to calculate the particle temperature, as most of the particle radiation was claimed to be soot radiation. A similar method was used by Thornock et al. [27] to study oxygen enriched combustion of biomass. Two-dimensional images were taken of the flames and the radiative intensity of the flames was determined by calibration with a black body oven. The temperature of the flame was then determined using the same method as Draper et al. [19] used. Also Tree and Peart [28] and later Stimpson et al. [29] worked with optical methods to study soot and char particles in flames of technical scale. They developed a two-color laser extinction method in which two wavelengths were used in the analysis of the transmitted radiation in order to be able to distinguish between soot and char particles. With this method it was possible to estimate the line-of-sight soot volume fraction in a coal fired flame. Andersson et al. [31] investigated radiative heat transfer in propane fired oxy-fuel flames and showed that the soot radiation may also be important for gas fired flames. In a later work by Andersson et al. [32], it was shown that the particle radiation constitutes a significant part of the total radiative intensity in the investigated lignite fired flames. Bäckström et al. [33] showed that the char or fuel particles are the main source of particle radiation in the examined lignite flame and that soot was a minor contributor to the particle radiation.

There are some studies where measurements of radiative heat transfer have been performed in large scale combustion facilities. Butler and Webb [34] performed heat flux and temperature measurements in a 80 MW_e coal fired boiler. Smart et al. [35] measured radiative heat flux in a 500 kW_{th} test furnace for different oxy-fuel cases for two coals and a similar study [30] was done but with co-firing of coal and biomass under oxy-fuel conditions. The influence from recirculation rate on the radiative heat flux was discussed, but no temperatures were measured. In common for these studies on radiative heat flux under various combustion conditions is that no radiation modelling was done. Therefore, it is difficult to conclude what causes the observed differences between the test cases.

In addition to experimental studies or, in a few cases, combined experimental and modelling studies there are also a number of theoretical works. In a modelling study by Mehta et al. [36] the radiation characteristics and turbulence-radiation interactions in lab-scale flames were investigated. Gas and soot radiation was modelled using detailed models, where the gas properties were based on line-by-line data and the soot properties were calculated from the Rayleigh theory. A photon Monte Carlo method was used to solve the Radiative Transfer Equation and it was concluded that soot emission can contribute with up to 70% of the total emitted radiation in the investigated flames. Marakis et al. [37] used a Monte Carlo approach and the P1 approximation to calculate the radiative heat transfer in a cylindrical coal fired furnace. They concluded that for strongly forward scattering particles, it might be more correct to neglect scattering than to assume iso-tropic scattering. The influence from the optical properties of the particles were also stressed, where the influence of unburned fuel in the ash were seen as an especially important future research area. Ahluwalia and Im [38] calculated the radiative heat transfer conditions in a 915 MW_{th} coal fired furnace using a band model for the gas properties, Mie-theory for the particle properties and accounted for the particle size distribution of particles. The furnace was divided into separate zones with assumed/calculated particle concentrations. Soot was in this study found to have a higher influence on the total heat transfer in the furnace than char particles. Mengüc and Viskanta [39] performed a parametric study in a coal fired cylindrical furnace. It was concluded that the number density, temperature and the distribution of particles in the furnace had a larger influence on the radiative heat transfer than the particle properties, *i.e.* complex index of refraction, and the gas concentrations.

The available literature on radiative heat transfer in rotary kilns is limited. Experimental studies are very challenging due to the limited access, but some modelling studies on radiation in rotary kilns are available [40-43]. Compared to the works on combustion in boilers, flame radiation in rotary kilns is treated with more approximate methods. Boateng [43], gives a review of the current modelling approaches of heat transfer in the freeboard of a rotary kiln. The presented models do, however, only consider gas radiation and no attention is paid to particle radiation. Also in the modelling studies by Gorog et al. [40] and Barr et al. [41] particle radiation was neglected.

1.3 Flame radiation studies at Chalmers

There are many studies presenting data of interest for analysis of flame radiation as presented above, *e.g.* studies on particle temperature using two-colour pyrometry, measurements of soot volume fractions in flames and particle concentrations in combustion chambers. But, there are few publications focusing on more than one specific aspect of the radiative heat transfer, and particularly few studies combining measurements with radiation modelling.

This work has an aim of combining radiative intensity measurements and comprehensive experimental data of other relevant parameters with detailed radiation modelling to study flame radiation and address questions that cannot be answered by measurements or modelling alone. Several measurement techniques are implemented in the methodology to minimize the assumptions needed in the modelling. The work presented in this thesis is focused on quantifying important parameters for the radiation, *e.g.* particle temperature and concentration. The methodology used in this work is a continuation of the work previously done at Chalmers where flame radiation has been studied during more than 10 years, which is shortly reviewed below. The first works combined narrow angle radiometer measurements and radiation calculations to study the radiation conditions of propane-fired oxy-fuel conditions [31, 44]. The difference between the modelled gas radiation and measured total radiation gave an indication of the particle radiation in the different flames. The first study including modelling of particle radiation investigated lignite flames [32] and the particle radiation was modelled as soot radiation only, *i.e.* scattering was not included. In the work by Johansson et al. [45-47], the radiation model was refined to also include large, scattering, ash and coal particles where the Mie-theory was used for calculation of the particle properties. With this model it was possible to calculate the particle radiation based on assumed concentrations of particles and particle temperatures in the flame. However, it was recognized that the results were sensitive to the assumed particle properties and that it was desirable to further develop the experimental methods and modelling to clarify the contribution of particle radiation. The work presented in this thesis therefore aims to develop the combined experimental and modelling methodology to be able to improve the quantification and characterization of particle radiation.

The narrow angle radiometer has been used as the reference measurement system in this work since it is an excellent instrument for studying the flame radiation without the influence from walls and other surfaces. The methodology applied in the works presented above has been developed by including additional measurement instruments in the experimental setup. Two types of instruments have been tested, an optical FTIR based technique (Paper I and IV) and several instruments for analysis of particles extracted from the flame (Paper II, III and V). These instruments provide information about the particle temperature, particle size distribution, particle concentration and particle type that had to be assumed or fitted in the previous studies. The radiation model has also been developed to analyse the new information gained, and to show the influence on the flame radiation from the different parameters. The main development steps can be summarized as follows: to be able to account for different particle and gas temperature (Paper I), and to be able to account for different particle types and size distributions (Paper II and V). The work has been focused on developing the methodologies, where the presented results can be seen as examples of possibilities for studies of flame radiation enabled by the suggested combination of measurement and modelling strategies. The strength when combining measurements with modelling, as done in this work, is that in addition to only presenting measurements of a single parameter, *e.g.* soot volume fraction, the influence on the total flame radiation can be shown as well. It is not the aim of this work to present general conclusions on *e.g.* soot formation in coal flames. Instead, the focus is to show how the influence of this type of parameters can be characterized in a flame of technical scale. As a continuation of this work, it will be interesting to apply the methodology in varying combustion conditions to find more general conclusions about the influence of particle radiation in flames.

1.4 Aim and Scope

The overall aim of the work presented in this thesis is to develop a methodology combining measurements and modelling where the relevant radiative heat transfer mechanisms active during combustion in flames can be quantified. A particular focus of the present thesis is the radiation emitted, absorbed and scattered by particles, both in gaseous and solid fuel combustion. Important factors which influence the total flame radiation have also been identified, and some of the most important factors have been investigated. The aim of this work can be divided into the following specific research questions:

- What is the role of particle radiation in the high temperature zone of a coal flame? (Paper I, II, III and V)
- Which measurement instruments are suitable for characterization of particle radiation in flames? (Paper I, II, III and V)
- What is the contribution from the different types of particles to the particle radiation? (Paper I, II and V)
- How does the particle type and size distribution influence the particle radiation? (Paper I, II, and V)

2. Thermal radiation in combustion

The following chapter presents the theoretical background used in this work to study radiative heat transfer in combustion applications. Radiative heat transfer is a mechanism, where electromagnetic waves transfer heat, mainly in the infrared region of the spectrum, 700 nm – 1000 µm, but also to a small extent in the visible and ultraviolet (UV) regions. The UV- and visible regions are mainly of interest in connection to various measurement techniques and do not contribute significantly to the heat transfer unless the temperatures are extremely high. Radiation is often characterized by its frequency, wavelength or wavenumber, denoted v, λ and η respectively. In this work the wavenumber, η, is most often used to describe the spectrally dependent radiation. The dependence on wavenumber and temperature of the emissive power, $E_{b,\eta}$, emitted by a blackbody is described by Planck´s law according to Eq. (2.1) [48].

$$E_{b,\eta} = \frac{C_1\eta^3}{\mathrm{n}^2\left[\exp\left({C_2\eta}/{\mathrm{n}T}\right) - 1\right]} \tag{2.1}$$

C_1 and C_2 are constants, T is the temperature and n is the refractive index, which is assumed to be constant and for gases (n ≈ 1).

The spectral blackbody radiation for three different temperatures in the IR-region is shown in Fig. 2.1a. In the figure it can be seen that the intensity is low in the visible region, 14285 - 25000 cm^{-1}, compared to the IR-region, at typical combustion temperatures. It is also seen that the peak of the curve is shifted towards higher wavenumbers, towards the visible region, when the temperature is increased and that the peak intensity increases significantly. The total emissive power, the integrated Planck-curve, is described by Stefan Boltzmann's law, Eq. (2.2) in which σ is the Stefan-Boltzmann constant. The total emissive power, E_b, is proportional to the temperature to the power of four, which stresses the importance of accurate information of the temperature to understand the radiative heat transfer.

$$E_b = \sigma T^4 \tag{2.2}$$

The spectral radiative intensity emitted by a blackbody, $I_{b\eta,}$, describes emitted radiation in a specific direction and is calculated from Eq. (2.3a), assuming diffuse emission, and its total counterpart is given by Eq. (2.3b).

$$I_{b,\eta} = \frac{E_{b,\eta}}{\pi} \quad (2.3a)$$

$$I_b = \frac{E_b}{\pi} \quad (2.3b)$$

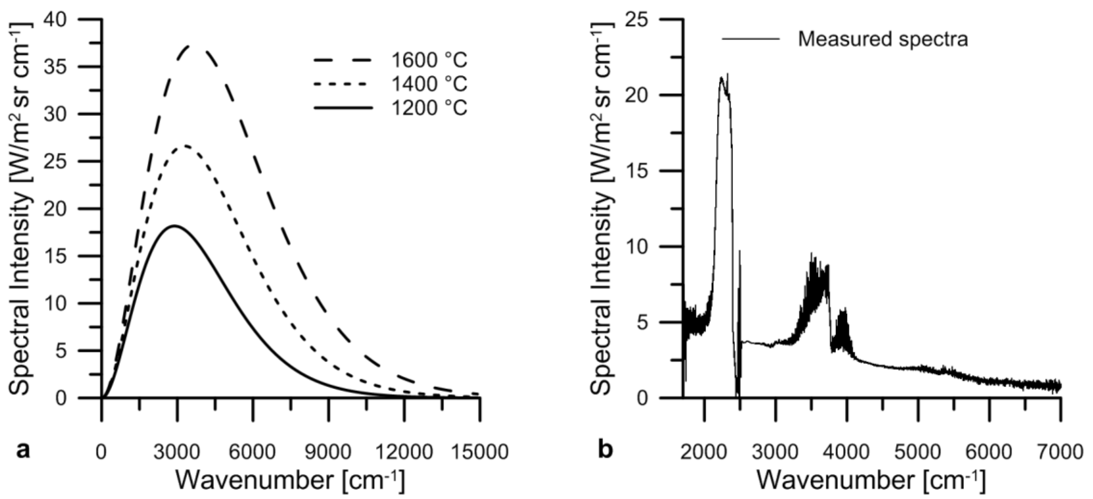

Figure 2.1. a) Planck curve for typical flame temperatures and **b)** example of IR-spectrum of gas- and particle radiation.

When radiation travels through a medium along a path which emits, absorbs and scatters radiation, the intensity of the radiation changes. This is described by the Radiative Transfer Equation (RTE), Eq. 2.4. Both gases and particles cause absorption, emission and scattering of radiation in a flame, as described by the RTE.

$$\frac{dI_v}{ds} = \kappa_g I_{b,v}(T_g) + \kappa_p I_{b,v}(T_p) - (\kappa_g + \kappa_p)\, I_v - \sigma_v I_v + \frac{\sigma_v}{4\pi}\int_0^{4\pi} I_v(\tilde{s}_i)\,\Phi(\tilde{s},\tilde{s}_i)d\Omega_i \quad (2.4)$$

The first and second term is the positive contribution from radiation emitted by gas species and particles respectively. The third term represents the decrease in intensity due to absorption of incoming radiation by gases and particles. The loss due to scattering of radiation into other directions is described by the fourth term, and the final term, the integral, describes the positive contribution from radiation scattered into the direction of interest from all other directions.

The spectral features of gas and particle radiation are fundamentally different due to their radiative properties and these are shortly described in the following section.

Gas radiation

Figure 2.1b shows a typical IR-spectrum consisting of both gas- and particle radiation. The parts of the spectrum with high peaks are regions where gas molecules absorb and emit radiation. The spectral emission and absorption by gases depend on the gas concentration and temperature. The two gases of most importance for heat transfer in combustion are H_2O and CO_2. The interaction between molecules and photons give rise to rotational and vibrational transitions in the molecules. For a gas, these transitions only occur at discrete wavenumbers. The transitional lines are normally very narrow, and the gas radiation is thus highly spectrally dependent. Each H_2O and CO_2 molecule absorbs and emits radiation in a large number of lines in the IR-region and these are grouped in so called rotational bands. This cannot be seen in Fig. 2.1b where closely spaced absorption lines of CO_2 (mainly around 2350 cm^{-1}) and H_2O (3000 – 4000 and around 5000 cm^{-1}) are merged into absorption regions, since the resolution of the spectrometer prevents individual lines to be resolved. These characteristics results in strong emission and absorption within the bands whereas the gas is non-active in the radiative heat transfer for the spectral regions between these bands.

Particle radiation

Fuel or char, ash and soot particles are present in a flame in various concentrations depending on the type of fuel, combustion conditions and position within the flame. In combustion of gaseous or liquid fuels only soot particles are present, while combustion of solid fuels results in a mixture of all particles. The spectral feature of particle radiation is, as noted, fundamentally different from gas radiation. The particles can be characterized as broad-band emitters, meaning that they emit and absorb radiation continuously in most of the spectrum. This can be seen in Fig. 2.1b, where there is a uniform background radiation from particles in the parts of the spectrum without gas radiation, *e.g.* 2500-2700 cm^{-1}. Large particles, such as fuel and ash particles, also scatter radiation in contrast to gases and small particles, which only absorb and emit radiation [48]. In pulverized coal combustion, particles in the size range 5 – 400 µm are fed to the burners [3]. The combustion of coal consists of three phases; drying/heating, devolatilization and char combustion. The first two phases occur near the burner whereas the char combustion requires longer time. The char/fuel particles are therefore most abundant in the flame region. Soot consists of small carbon containing particles formed from hydrocarbon molecules in fuel rich regions of a flame. Soot particles are significantly smaller than coal and ash particles, with a typical size of 25 – 65 nm for coal derived soot [25]. The amount of soot formed is highly dependent on fuel type and on combustion conditions [30]. In the post flame zone and in recirculation zones, ash particles are the dominating type of particles. Ash particles consist of the non-combustible components in the fuel such as metals. These components are either vaporized and later condensed or left as solid phase components after the char is combusted. The size of the ash particles typically varies from submicron particles up to tens of µm [49].

The absorption and scattering coefficient of a cloud of spherical particles with uniform radius, r_p, and number density, N_T, can be calculated using Eqs. (2.5) and (2.6).

$$\kappa_\lambda = \pi r_p^2 N_T Q_{abs} \tag{2.5}$$

$$\sigma_\lambda = \pi r_p^2 N_T Q_{scat} \tag{2.6}$$

Where the absorption, Q_{abs}, and scattering efficiency, Q_{scat}, depends on the particle type and size and is often calculated with the Mie-theory. The calculation of the gas and particle properties and the solution of the RTE are presented in Chapter 5.

3. Measurement techniques for radiation applications

This chapter presents a review of measurement techniques which can be used to study radiation and parameters influencing the radiation such as temperature and particle type and concentration. In general, there is a clear correlation between the scale of the combustion and the complexity of the measurement equipment that can be used. In lab scale applications the most advanced techniques can be applied, whereas in full scale coal combustion furnaces the possibilities of performing detailed measurements are very limited. The overview of measurement techniques presented here is focused on techniques applicable to technical, pilot and full scale facilities. However, in recent years there is a tendency of applying more advanced, sometimes even laser based, techniques also to full scale applications [50]. But laser measurements in the flame zone of larger combustion chambers are still scarce. The techniques presented here do not cover all possible techniques, but should be regarded as an overview of interesting techniques that can be used to analyze radiative heat transfer conditions in flames. Chapter 4.3 shows which of the presented techniques that have been used in this work. Apart from measurements of the radiative properties, intensity and flux, temperature is the most critical parameter to determine to obtain a good understanding of the radiative heat transfer. Accurate measurements of gas concentrations in the flame are also important for modelling of the gas radiation, but since this work focuses on particle radiation, the presented techniques rather concern measurements of particle concentrations. Measurements of gas concentration are relatively straight forward, where standard instruments for gases like CO_2, CO and O_2 can be applied. Measurement of H_2O is more challenging but with an FTIR instrument it is possible to measure also the water concentration with high accuracy.

The scale of a combustion facility is called various things in the literature, *e.g.* lab, small, technical, pilot and full scale. For clarity, flames with a thermal input of approximately 1 – 10 kW are in this work called lab or small scale. Flames larger than 50 kW are termed technical or pilot scale. Full or large scale refers to utility boilers with sizes up to several GW_{th}.

3.1 Radiative intensity

Measurements of the radiation intensity can be performed with a Narrow Angle Radiometer, which is a measurement technique developed by the International Flame Research Foundation (IFRF) [51]. The radiation is collimated using a long tube placed in a water cooled probe. The probe can be inserted into a flame and the radiation emitted along a line-of-sight path in the flame, which is aligned with the inner tube will reach a detector in the back-end of the probe. The research group at Energy technology at Chalmers have used a probe inspired by the IFRF design and developed the design further to the probe used in this work which is shown in Fig.

3.1 [31, 32, 44, 52]. The water cooled probe is approximately 2.4 m long and the inner diameter of the collimating tube is 10 mm. This implies that the angle of the collimated beam of radiation is very narrow. The detector is placed in a water cooled jacket with a separate water cooling circuit to maintain a constant temperature in the detector housing. The detector is a thermopile, which is a broad-band thermal detector with a time constant in the order of 0.1 – 0.01 s. The sampling frequency used in the measurements is 100 Hz, which means that some of the turbulent temporal fluctuations in the flame can be captured and an approximation of the intensity fluctuations can be obtained using this detector. The spatial resolution is, however, limited as the measurements only give line-of-sight averages. The detector is calibrated in a precision black body oven (Landcal R1500T) up to 1500°C, which corresponds to an intensity of 178 kW/m^{2}sr. During experiments in Chalmers 100 kW oxy-fuel rig the intensity is measured against a cold background in form of a window. The Narrow Angle Radiometer therefore provides excellent data on flame radiation only, since the cold background diminishes the influence of wall radiation.

Other techniques to measure the radiative intensity also exist. One example is to use a CCD camera to approximate the intensity by digital imaging [27]. In these measurements each pixel of the camera sensor represents a small part of the total image, and a value of the intensity corresponding to each pixel can thus be obtained if the camera is calibrated with a blackbody. The advantage of such a technique is that a 2D image of the flame/surface is obtained while traversing in-flame measurements are more problematic due to the size of the camera which would have to be mounted inside a water cooled probe to be able to be placed inside the flame.

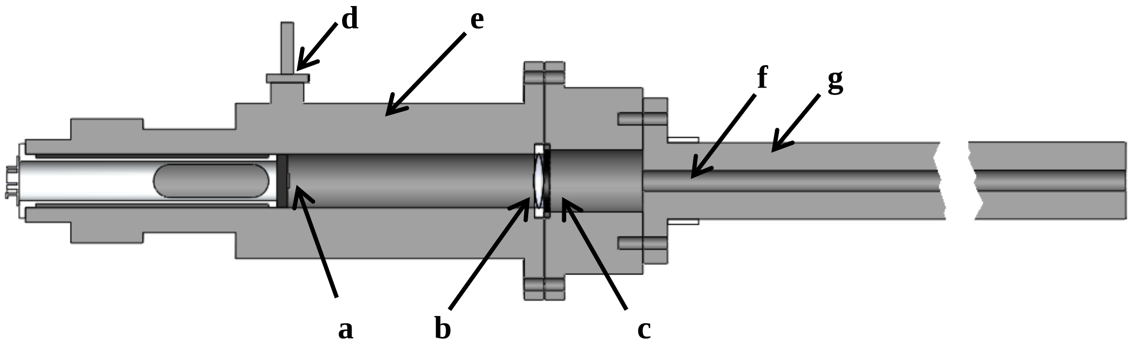

Figure 3.1. Schematic of the narrow angle radiometer which was used to measure the total radiation intensity. The probe includes the following components: **a)** thermopile, **b)** focusing lens, **c)** shutter, **d)** PT-100, **e)** water cooled sensor housing, **f)** collimating tube and **g)** water cooled probe.

3.2 Radiative heat flux

In some cases it might be interesting to investigate the incident radiation on a wall, for example in comparison with CFD calculations or design of heat transfer surfaces. In that case a detector which collects radiation from all angles is used. An example of such an instrument is the ellipsoidal radiometer, Fig 3.2. This device collects radiation from a large part of the hemisphere. The instrument is mounted in the tip of a water cooled probe, and by aligning it with *e.g.* a boiler wall it is possible to measure the incoming radiative heat flux to the wall. Total heat flux probes are sometimes used for this purpose, these probes consist of a metallic surface in which thermocouples are inserted at different distances from the surface. By calculating the temperature gradient, it is possible to measure the conducted heat in the metal and thus the total heat transfer from the surface. Examples of studies of measuring radiative heat flux in flames are Refs. [17, 34, 35, 53].

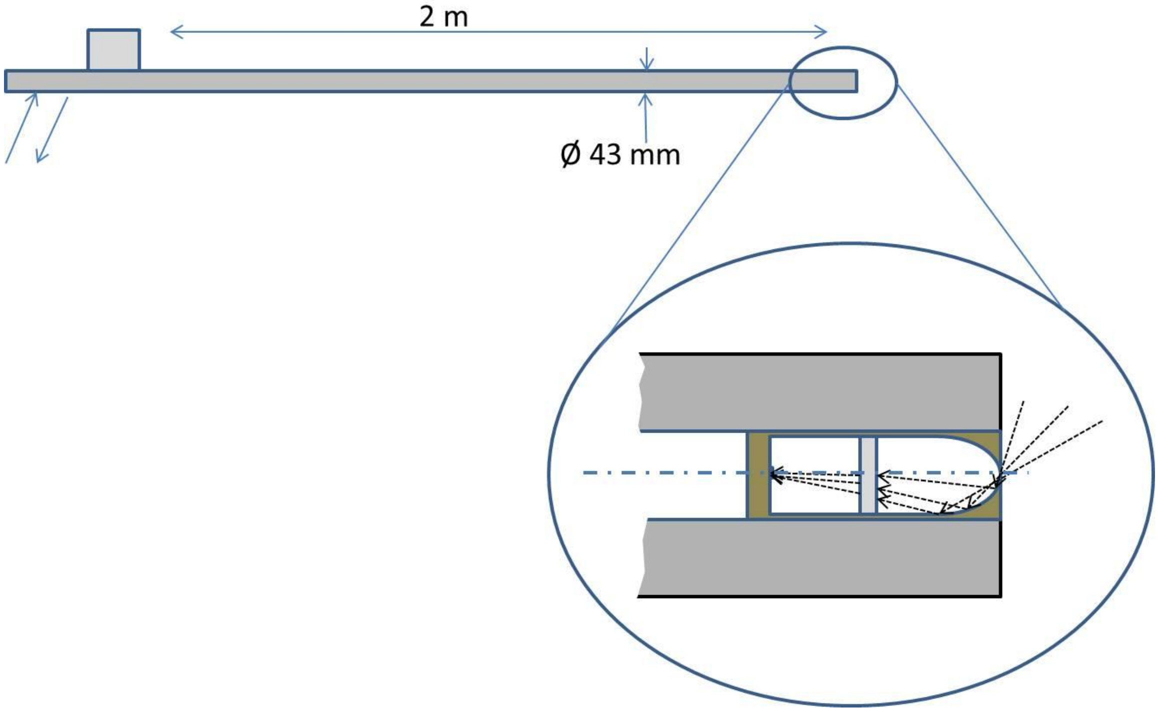

Figure 3.2. Principle schematic of a radiative heat flux probe. The magnified figure shows the ellipsoidal radiometer mounted in the probe tip**.**

3.3 Spectral radiation

An instrument measuring spectrally resolved radiation provides additional information that cannot be obtained with the total radiation techniques. Instead of a detector measuring only the total radiation, a spectrometer can be used to record the infrared spectrum. A common technique for gas concentration measurements is the Fourier Transform Infra-Red (FTIR) spectrometer. However, FTIR spectrometers have also been used for radiation measurements in flames [13, 22-24, 33]. If the detector in the FTIR covers a broad spectral region it is possible to integrate the measured spectrum and obtain the total intensity. But, the detectors commonly used in FTIR (DTGS, InSb, MCT) covers a part, but not all, of the infrared spectrum and the instruments are often used for other purposes, *e.g.* gas or particle temperature measurements, than to measure the total radiation. Early works using FTIR to measure radiation in flames positioned the spectrometer close to a small flame and collected the emitted radiation from the flame directly [14]. This procedure gives information about line-of-sight properties in the optical path seen by the spectrometer. In a more recent application, developed by Clausen et al. [54] and Bak and Clausen [22], a water cooled probe was equipped with fibre optics to enable in-flame measurements of the spectral radiation.

With this technique a higher spatial resolution can be obtained. As for the other radiation measurement techniques, a calibration procedure is needed to obtain the spectral intensity, and this is done by using a black-body with known temperature and emissivity.

Other types of spectrometers can be used [21], but in the FTIR-based techniques it is the spectral features in the IR region that are used to determine the temperature of gases and particles. Normally, the strongly absorbing region of CO_2 around 2350 cm^{-1}, which even for a short path length acts as a black-body, is used to determine the gas temperature. A Planck-curve representing the gas temperature can be fitted to this spectral region to estimate the gas temperature, Fig. 3.3d. To determine the emissivity and temperature of particles a grey body curve, representing the particle radiation, can be fitted to the regions without gas absorption, Figs. 3.3a – c. Since a broad spectral region is used, it is possible to fit both the temperature and emissivity of the grey Planck-curve to these spectral regions without knowing the emissivity of the object.

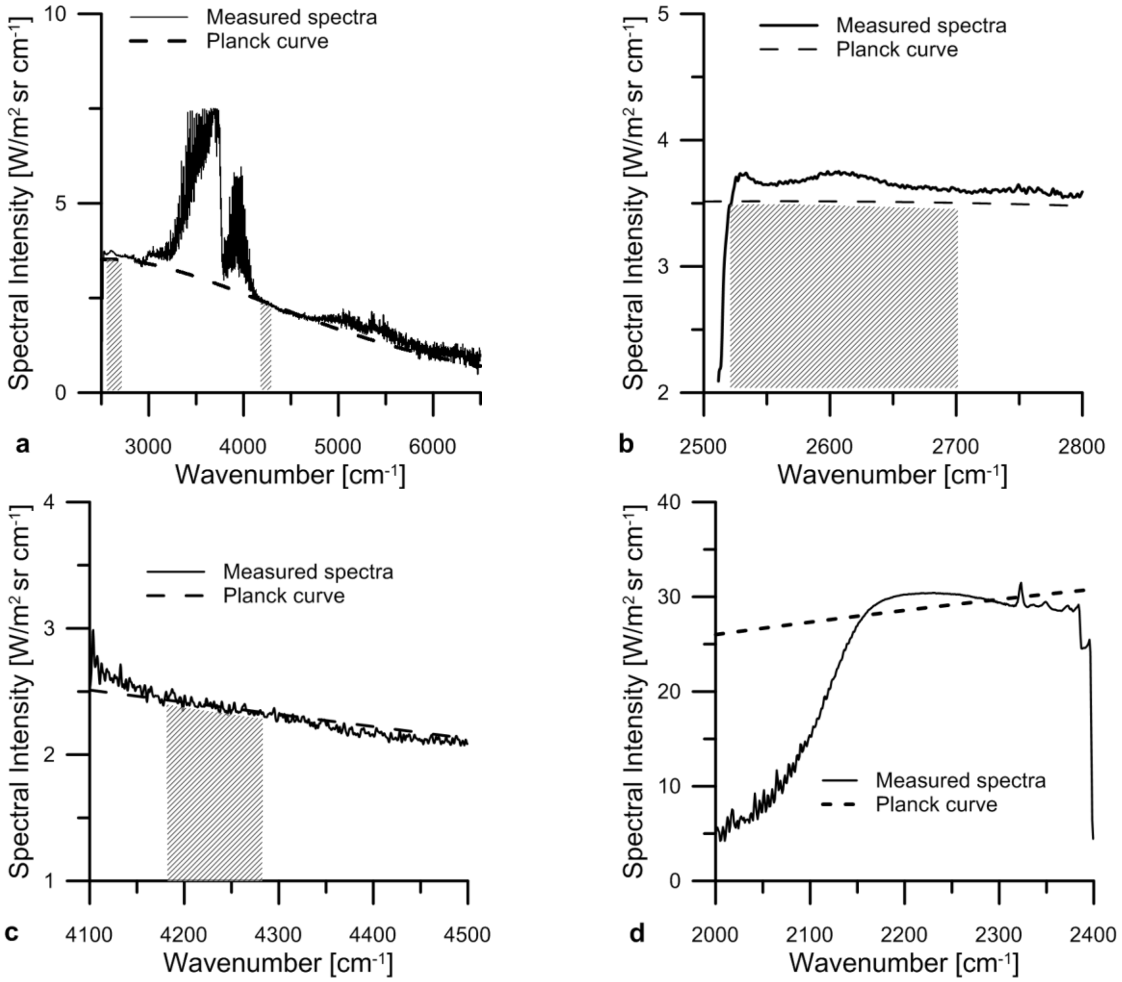

Figure 3.3. Measured spectra and fitted grey- and black body radiation. **a)** Areas (shaded) used when fitting the grey body to the measured spectra. **b)** and **c)** zoomed areas of interest. **d)** The strongly absorbing region for CO_2 around 2350 cm^{-1} which can be used to determine the gas temperature by fitting a black-body curve to the measured spectrum in this region.

3.4 Temperature measurement techniques

Temperature is, as discussed previously, a critical parameter in radiative heat transfer and it is therefore of utmost importance to be able to measure particle- and gas temperatures accurately in experimental studies of radiative heat transfer. Available temperature measurement techniques applicable to flames of the scale investigated in this work are shortly reviewed below. Some of the techniques enable simultaneous measurements of temperature and particle concentration.

Thermocouples

Thermocouples are often used to measure the temperature in combustion applications due to their high permissible working temperatures and low cost. The materials used in thermocouples are rare metals and two common thermocouples in measurements of flame temperature are Type S and Type B, which both consists of platinum and rhodium. The maximum temperature that can be measured with these thermocouples is 1480 and 1700°C respectively. A simple way of measuring temperature is to use a bare thermocouple inserted into the flame. This technique is often used in lab-scale flames or in applications with moderate temperatures. One of the main problems with this technique is that at high temperatures the radiative loss from the thermocouple becomes large and this loss will influence the temperature of the thermocouple and measurement accuracy.

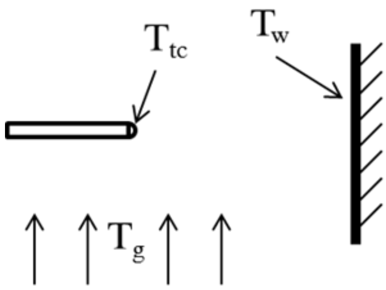

Figure 3.4. Schematic figure of a thermocouple in a gas stream close to a wall.

Figure 3.4 shows a schematic of a thermocouple inserted into a gas stream with a temperature, T_g, close to a wall with a temperature, T_w. From the temperature measured with the thermocouple, T_{tc}, it is possible to get an estimation of the gas temperature by solving an energy balance for the thermocouple according to Eq. 3.1.

$$h\left(T_g - T_{tc}\right) = \sigma\varepsilon(T_{tc}^4 - T_w^4) \tag{3.1}$$

which, after rearrangement, yields the following expression,

$$T_g = T_{tc} + \frac{\sigma\varepsilon(T_{tc}^4 - T_w^4)}{h} \tag{3.2}$$

where ε is the emissivity of the thermocouple and h is the convective heat transfer coefficient describing the heat transfer between the thermocouple and the gas stream. In this simplified case, all walls surrounding the thermocouple are assumed to have the same temperature but in a real case these surfaces usually have different temperatures. Also, the surrounding gas and particles absorb and emit radiation between the walls and thermocouple making the analysis more difficult. The emissivity of the thermocouple changes if deposits are formed on the surface, the emissivity also changes with temperature and can vary up to 40% for temperatures in the range 600 – 900°C [55]. Further, the velocity and gas properties have to be known to estimate the convective heat transfer. In summary, it is possible to correct for the losses and a reasonable accuracy can be obtained if the boundary conditions are well known, but often this is not the case and more advanced techniques have to be applied to obtain satisfactory measurement accuracy.

The suction pyrometer

In order to avoid the radiative loss from unshielded thermocouples a so called suction pyrometer is commonly used in combustion applications of technical to industrial scale. The suction pyrometer is a robust and relatively simple technique. In a suction pyrometer, the thermocouple is shielded by ceramic tubes, and the flue gas is sucked with a high velocity between the ceramic tubes, up to 200 m/s is required [55]. An example of a triple-shielded suction pyrometer used for temperature measurement in coal flames is shown in Fig. 3.5, the thermocouple is mounted so that the tip of the thermocouple is positioned close to the tip of the inner shield. The flue gas is sucked through a hole in the outer shield and then it passes through small channels between the inner and middle shield with a high velocity. The convective heat transfer is then increased at the same time as the radiative losses are suppressed so that convection entirely dominates the radiative heat transfer and the thermocouple will attain the same temperature as the gas. This can be understood from Eq. 3.2 as an increase in the convective heat transfer, h, coefficient will decrease the influence from the second term on the right hand side.

The problem with the suction pyrometer is that it is an intrusive measurement technique and that a relatively large volume flow needs to be extracted from the flame to obtain the high velocity required. The extraction of gas from the flame will therefore affect fluid dynamics and stoichiometric conditions and this influence becomes of particular importance in small-scale flames. The use of suction pyrometers in small flames is thus limited, and they are more suitable for flames of industrial scale. The spatial resolution of the measurements is determined by the amount of gas extracted from the flame, and the measured temperature is an average of the gas and particle temperature in the measurement volume created by the suction velocity. Another difficulty when measuring with suction pyrometers in particle dense flames is the build-up of particles between the ceramic shields which decreases the velocity which also dampens the effectiveness of the convective heat transfer. At high temperatures and high ash concentrations, ash melting will also be a problem. The melted ash will condense on the ceramic shields and eventually melt them together, thus destroying the shields since the melted ash deposits are difficult to remove. The measurement equipment also has a high thermal inertia, which prevents measurements of fast temperature fluctuations in the flame.

The expected accuracy of the average temperature measured with a suction pyrometer is +/-50 K provided that a sufficiently high suction velocity is obtained.

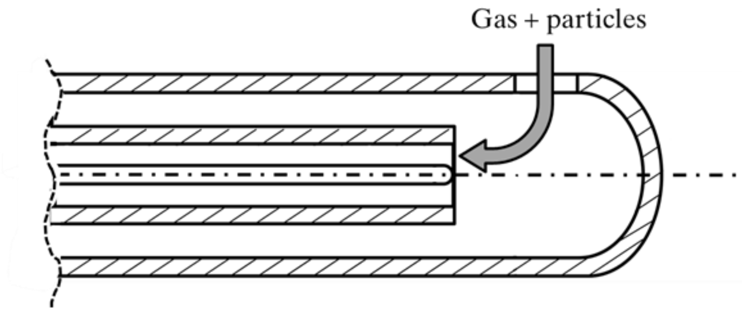

Figure 3.5. Example of a triple-shielded thermocouple used for temperature measurements in coal flames. The ceramic shields are mounted in the tip of a water cooled probe and the thermocouple is mounted inside the inner shield.

Optical pyrometers

A traditional non-contact technique for estimating the surface temperature of an object is to visually observe its colour. This is an old technique which has been utilised extensively to get a rough estimation of the surface temperature of objects over about 700°C [56]. Techniques that measure the radiative intensity in a specific wavenumber interval of the radiation emitted from a surface to determine its temperature are referred to as pyrometry. Radiation emitted by a surface depends on the temperature and emissivity of the surface. The temperature of the surface can be calculated from the Planck-curve when the emissivity of the object is known. Radiation emitted from the investigated object is filtered so that only a specific wavelength is measured. By calibrating the pyrometer with a radiation source with known emissivity, e.g. a black body oven, the measured intensity of the filtered radiation can be related to the Planck-curve and the temperature can be calculated. Simple hand-held instruments used to measure surface temperature, so called IR-thermometers, are based on this technique, but knowledge about the emissivity of the measurement object is needed.

In combustion applications pyrometric techniques can be used to measure both gas and particle temperature, but requires knowledge of the spectral emissivity of the measurement target. To measure the particle temperature in flames the amount of particles has to be high enough for the particle cloud to act as a black body, i.e. the emissivity is close to unity within a volume of uniform temperature. To estimate the particle temperature in conditions with smaller amounts of particles is more difficult due to the problem of determining the emissivity and uncertainties in the background radiation. The gas temperature can be measured utilizing the spectral absorption features of the CO_2 in the flue gas, as previously described.

Two-colour pyrometry

When the emissivity of the measured object is unknown, simple pyrometric techniques cannot be used, but two-colour pyrometry may instead be an option. In two-colour pyrometry, two wavelengths, normally in the visible part of the spectrum, are used to determine the temperature of the object. Two-colour pyrometry has previously been used both in small scale combustion applications but is now also used to measure particle temperatures in pilot scale applications [17-19, 26]. For measurements of the particle temperature in a furnace the wavelengths should be selected so that they do not interfere with gas absorption bands. The emissivity of the particles is assumed to be the same for both wavelengths and the temperature of the particles can then be calculated from the ratio of the intensity of the two wavelengths without knowledge of the exact value of the emissivity. As for the "one-colour" pyrometer technique, calibration to a source with known temperature and emissivity is needed. It is also possible to use a non-gray emissivity of the particles when calculating the temperature, for example to account for the non-gray absorption by soot particles [19], although this requires some knowledge about the spectral dependence of the emissivity. In the early applications of two-colour pyrometry [56] the measured radiation was split and filtered and the two colours/wavelengths were measured with two separate detectors, Fig. 3.6. However, the development of CCD cameras has simplified the use of this technology. Each pixel with its colour filter in the camera can work as a sensor and this enables 2D pictures of the flame temperature [18, 19]. The same measurement principle but using three wavelengths, called multi-colour pyrometry, also exist [57, 58].

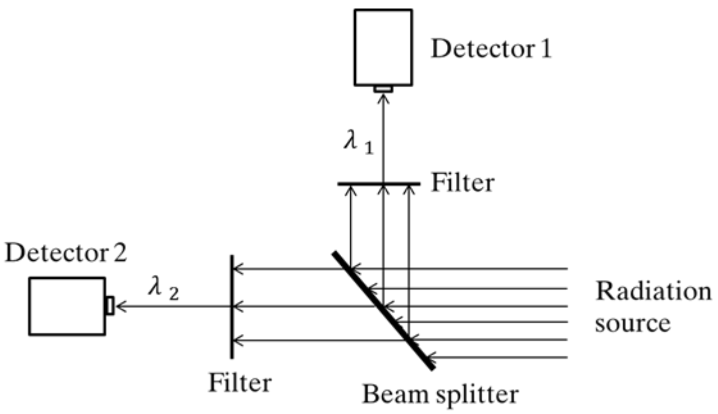

Figure 3.6. Schematic setup for two-colour pyrometer measurements using two detectors.

Laser based techniques

Laser techniques developed for combustion diagnostics are excellent tools to study detailed phenomena in flames. Both temperature and the concentration of gas species and particles can be measured with high spatial and temporal resolution. However, the applicability of these techniques in large flames is often limited by *e.g.* the limited optical access, beam attenuation by particles, fouling of windows and vibrations. Laser techniques are therefore rarely used in large scale combustion, especially not in solid fuel flames. Some examples of measurements in large scale experiments exist [50, 54, 59], but they are often carried out in the post flame zone. The difficulties with these techniques have to be solved before true point measurements with high temporal resolution in industrial scale flames can be realized. The field of laser diagnostics is vast, and many different techniques exist where the temperature can be determined. The temperature is often a fitting parameter when using techniques mainly intended for other purposes such as measurement of the gas species, with *e.g.* Laser-Induced Flourescence (LIF). But, the technique shortly presented below (CARS) is recognized as the most interesting for temperature measurements in large scale applications [50].

For gas temperature measurements, Coherent anti-Stokes Raman Spectroscopy (CARS) is commonly applied [50, 60]. In CARS measurements, three high-intensity laser beams are used to create a fourth beam, the anti-Stokes beam. The fourth beam is created in the intersection of the three other beams, which means that the spatial resolution in this technique is high. The created laser beam contains information about the temperature of the gas species in the measurement volume created by the intersection of the tree original beams [60]. Figure 3.7 shows a schematic picture of the setup of the different beams in a CARS-system. There are some examples of where CARS have been used in coal flames of technical size [54, 59].

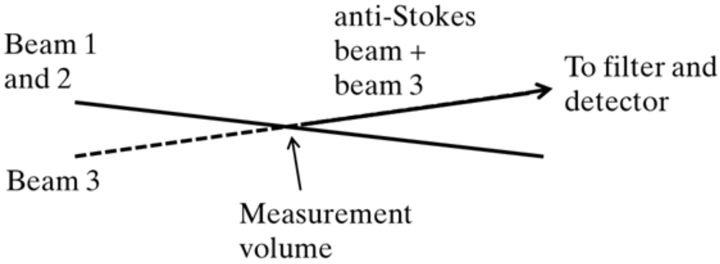

Figure 3.7. Schematic picture of the laser beams in a CARS-system.

3.5 Particle concentration measurements

Most of the techniques for measurements of particle concentration presented here are based on physical extraction of particles from the flame since this is the most common approach for analysis of particles in larger flames. The extraction of the particles is performed with a probe that is inserted into the flame and the particles can then be analyzed outside of the combustion chamber in a much more controlled environment. Examples of an extraction probe can be seen in Fig 3.8. The concentration of various particles in the flame is changing throughout the combustion process, *e.g.* soot particles are formed and or oxidized, ash components can be vaporized and condensed and char particles are combusted. To obtain a good measure of the particles in the position from which the gas is extracted it is essential to quench the reactions quickly in the probe. This is normally done by cooling the gas and particle mixture by adding an inert gas, such as N_2, thus diluting and cooling the sample gas. Also, the probe itself provides cooling since the probe is often cooled by water or oil and the temperature of the probe is thus significantly lower than the flame temperature. The aim is to have the same suction velocity of the gas into the probe as the flame velocity, so called isokinetic sampling. It is, usually, very difficult to accomplish isokinetic conditions, partly due to that the gas velocity in the flame rarely is known. It has, however, been shown that isokinetic conditions is not necessary to obtain a good approximation of the particle concentration, but rather to have a high enough suction velocity [61]. A very good control of the flows (dilution and sampling gas) is needed to obtain a good accuracy in the final results, especially if the sample flow is low.

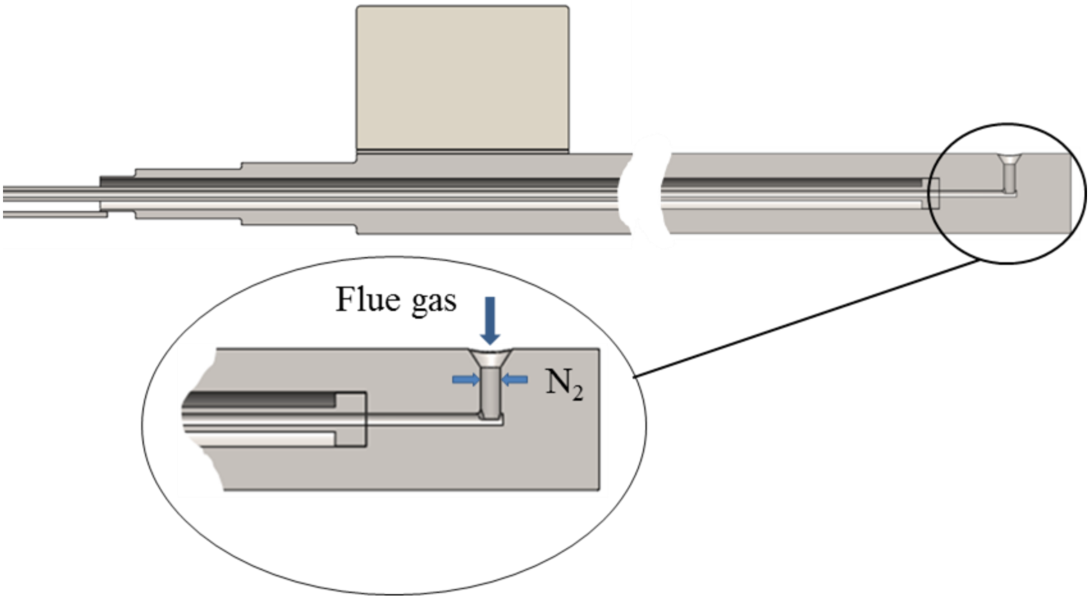

Figure 3.8. Water cooled probe used for extractive particle measurements. The total length of the probe is 2 m with an outer diameter of 43 mm. The diameter of the inner tube is 6 mm.

Filters

Probably the least complicated method to estimate the total mass concentration of particles is to collect the extracted particles in a filter. The filter can be made of materials such as sintered metal or fabric, depending on temperature and desired collection efficiency (pore size of the filter). By weighing the filter before and after the measurements the total mass of particles can be determined.

Cyclones

Small cyclones can also be used to separate particles from the sampled gas stream. The principle of a cyclone is that particles are separated from the gas based on their different mass by centrifugal forces created by circulating the gas inside the cyclone. The cyclones can be designed to separate particles larger than a certain diameter (assuming a certain particle density) for a known gas flow. Particles that hit the cyclone wall fall down and are collected in the bottom of the cyclone. The size distribution of the collected particles can be analyzed after the measurements if the total particle mass is sufficiently high. Several cyclones with different cut-off diameters can be used in series to obtain a crude particle mass distribution.

Low-Pressure Impactor

Low Pressure Impactors are used to size segregate particles based on their aerodynamic diameter. The most common impactor today is the Dekati Low Pressure Impactor (DLPI) which yields a particle size distribution of 13 stages between 30 nm and 10 µm. The separation of the particles is a result of different velocities in the stages of the impactor. The last stage of the impactor creates a large pressure drop, which acts as a critical orifice and determines the flow through the impactor. The DLPI is calibrated at room temperature and the flow is known from this calibration. The DLPI can be heated to avoid condensation, but the flow is then corrected to account for the elevated gas temperature. The mass of the collected particles on each stage is weighed, and from this information a particle size distribution is obtained. Extractive measurements using impactors have previously been used to study combustion generated particles in *e.g.* Refs. [7-11].

SMPS

A Scanning Mobility Particle Sizer is an instrument used to measure a high resolution particle size distribution of particles smaller than 1µm. The SMPS consists of two parts, a Differential Mobility Analyzer (DMA) where particles are charged from a radioactive source. The charged particles are then separated based on their electrical mobility when applying a voltage over the sampled gas [62]. Particles with a specific diameter are separated from the rest of the sample and can be counted in a Condensational Particle Counter (CPC) where iso-butanol is sprayed into the sample and the aerosols grow so that they can be counted. Figure 3.9 show a principle sketch of the SMPS instrument including DMA and CPC. The SMPS instrument is commonly used in aerosol measurements in the atmosphere [63], but some examples of when SMPS is used in combustion application also exist [52, 64].

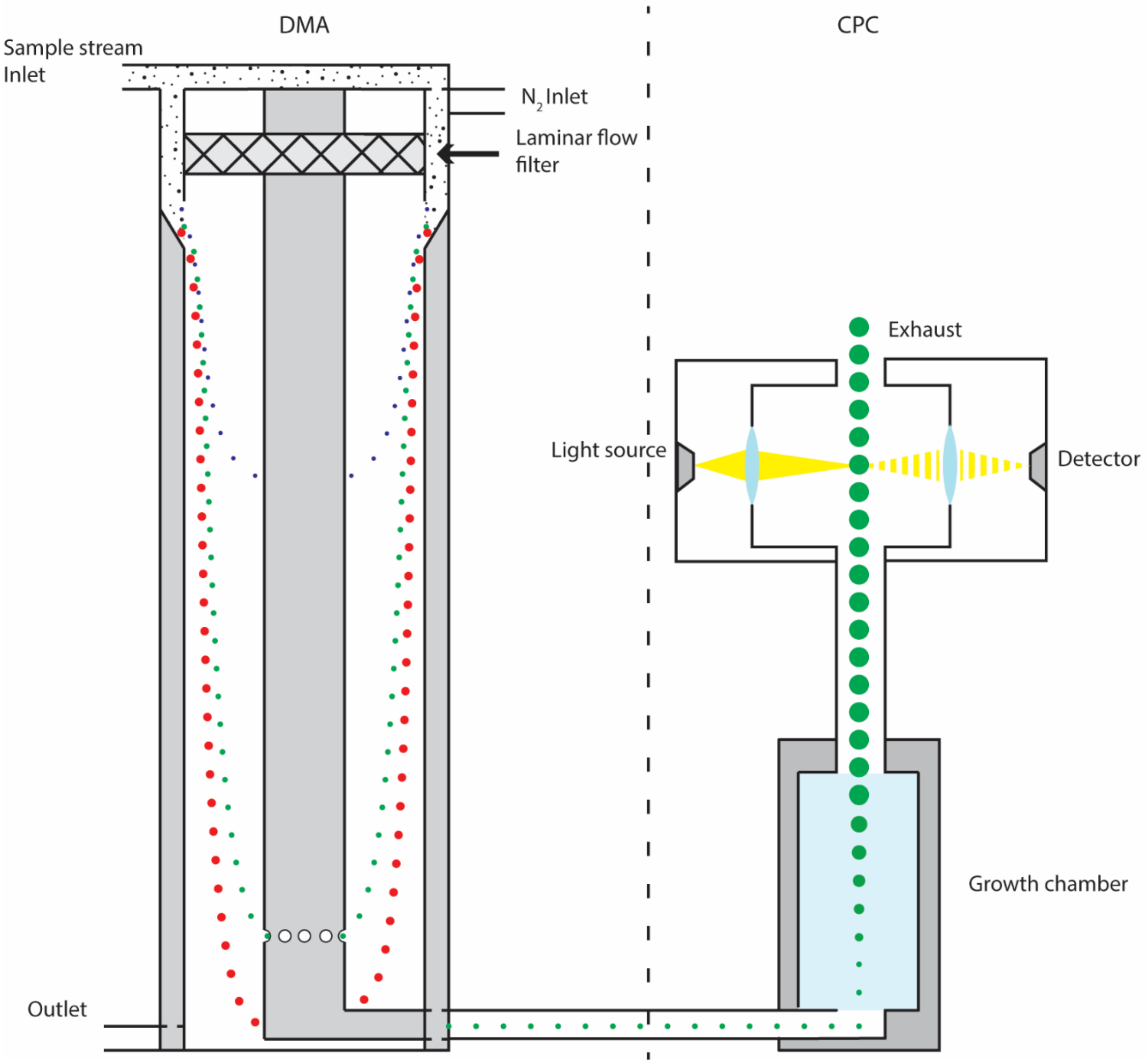

Figure 3.9. Principle sketch of the SMPS instrument including DMA and CPC.

Laser Techniques
As indicated earlier, laser techniques are versatile and can be used for simultaneous measurement of both temperature and concentration of gases and particles. In this section, techniques mainly intended for measurements of particle concentration are presented.

Laser Doppler Anemometry (LDA) is a well-established technique for measurement of velocity. The technique is based on two intersecting laser beams creating a measurement volume. When particles are passing through the measurement volume the beams are disturbed. Each particle is counted and from this information it is possible to estimate the local particle concentration and also velocity of the particles. There is an interference effect created by the particles, which can be used to calculate the size of the particle passing the volume as well. A similar technique was used by Black and McQuay [65] to measure the particle size and concentration in the radiant section of a 160 MW_e boiler.

Laser extinction/transmission measurements can also be used to estimate the soot volume fraction. A laser beam is then transmitted through the measurement volume/flame and from the radiation absorbed along the path of the laser beam the extinction coefficient (absorption + scattering coefficient) is calculated with Beer-Lamberts law. Examples of application of laser extinction to measure particles in flames of technical scale are few [28, 29], whereas the use of the technique in lab flames is extensive [50, 66-68].

For measurements of the soot volume fraction, the Laser Induced Incandescence (LII) technique is often used [50, 68-71], although it mainly concerns lab-scale flames. In LII, the soot particles in the flame are illuminated with a high powered two-dimensional sheet of laser. When the soot particles absorb the high intensity laser light they are heated to a temperature of approximately 4000 - 5000 K, due to which they start to emit radiation of high intensity. The emitted radiation is measured and related to the soot volume fraction via a calibration procedure in a well characterized reference flame. There are examples where laser extinction is used together with LII to avoid the calibration procedure [69]. Other studies have shown that the decay of the LII signal is proportional to the size of the particles [70, 71], and it is therefore also possible to obtain information about the size of the soot particles.

3.6 Particle property measurements

As recognized by Viskanta et al. [7], there are large uncertainties in the optical properties of the particles. Several studies have been devoted on deriving the complex index of refraction for different particle types, see *e.g.* Refs. [72-79]. These measurements are often very detailed and the theory behind the calculation of the complex index of refraction is complicated. It is therefore desirable to have a tool for validation of the calculated models. One instrument with the possibility of measuring both the absorption and scattering coefficient is the Photo Acoustic Spectrometer (PASS-3) [80]. This instrument has been developed with the aim of characterizing aerosols in the atmosphere. However, the instrument can likely also be used in combustion application. Considering the uncertainty in the particle properties, it is interesting to test an instrument with the possibility of measuring both the absorption and scattering coefficient by particles. It can therefore be used to evaluate the different complex index of refraction for different particle types. The measurement principle is that three laser beams with different wavelengths are applied to a soot/gas mixture, Fig. 3.9. The particles absorb the radiation and are heated, the heat is then transferred to the gas and the thermal expansion of the gas produce a sound wave which can be correlated to the absorption via calibration. A nephelometer is used to measure the scattered laser light, the scattered light is then used to calculate the scattering coefficient.

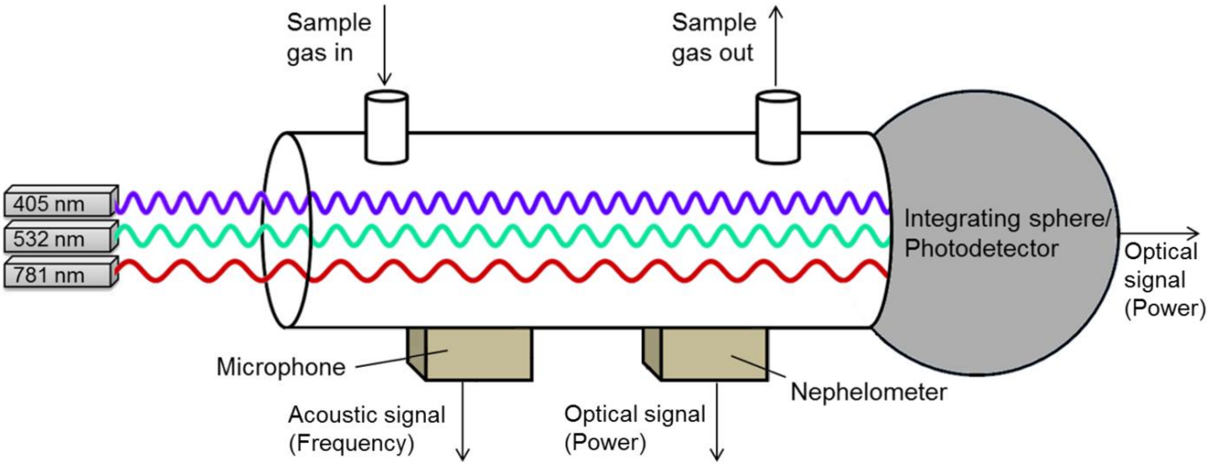

Figure 3.10. Schematic figure of the photo acoustic spectrometer (PASS-3).

4. Experimental facilities

The experimental work presented in this thesis has mainly been performed in two experimental units: the Chalmers 100 kW_{fuel} oxy-fuel test rig and the 400 kW_{fuel} Experimental Combustion Furnace (ECF). The majority of the experiments have been performed at Chalmers (Papers I-IV) and one experimental campaign was performed in the ECF (Paper V).

4.1 Chalmers 100 kW oxy-fuel test rig

The Chalmers oxy-fuel test rig is a 100 kW test furnace, which has been used for studies of various combustion related topics for the last 10 years [31-33, 52, 81, 82], with several studies related to radiative heat transfer as described in Chapter 1.3. It is possible to use either gaseous or solid fuels, propane and lignite have been used in this work. The combustion chamber is cylindrical with an inner diameter of 0.8 m and a height of 2.4 m. The walls are refractory lined and un-cooled, but to control the flame temperature four cooling rods are inserted into the furnace where water are used for cooling. The burner, consisting of replaceable fuel and air registers, is mounted on the top of the furnace. It is a swirling type burner with two air registers. In normal operation 40% of the air is supplied in the primary air register with a swirl angle of 45°, while 60% of the air is supplied in the secondary air register with a swirl angle of 15°. A refractory quarl has been installed near the burner, see Fig. 4.1, which was not used in previous studies by Andersson et al. [31, 32, 44], and the results from this study and the previous works are therefore not comparable in all cases. The burner and fuel registers used for the lignite fired experiments is also new compared to the one used earlier [32]. The fuel is supplied by a gravimetric coal feeding system to an annular register placed in the burner, Fig. 4.2. The gas burner used for the propane fired experiments is a bluff-body stabilized burner. A schematic figure of the gas burner can be found in the work by Hjärtstam et al. [83].

The unit can be operated in both air- and oxy-fired mode. During oxy-fuel operation flue gases are recycled in either dry or wet form, *i.e.* before or after the flue gas condenser. Oxygen from bottles are mixed with the recirculated flue gases before the primary air fan to obtain well mixed conditions before supplying the gas to the burner. The furnace is operated at a slight excess pressure, which prevents air ingress when operating in oxy-fuel mode. The CO_2 concentration on dry basis is normally 90 - 95% in the stack. Radial flame measurements are possible to perform in seven measurement ports (M1-M7) distributed along the height of the reactor. Quartz windows are placed on the opposite side of the furnace serving as a cold background in the measurements of radiative intensity and for visual inspection of the flame. It is possible to use two ports in 90° angle to the displayed measurement ports in the figure, but these ports are today used to monitor the wall temperature with thermocouples placed inside a refractory material. Both air fired and oxy-fuel conditions with dry and wet recycling were studied in this work for both propane and lignite.

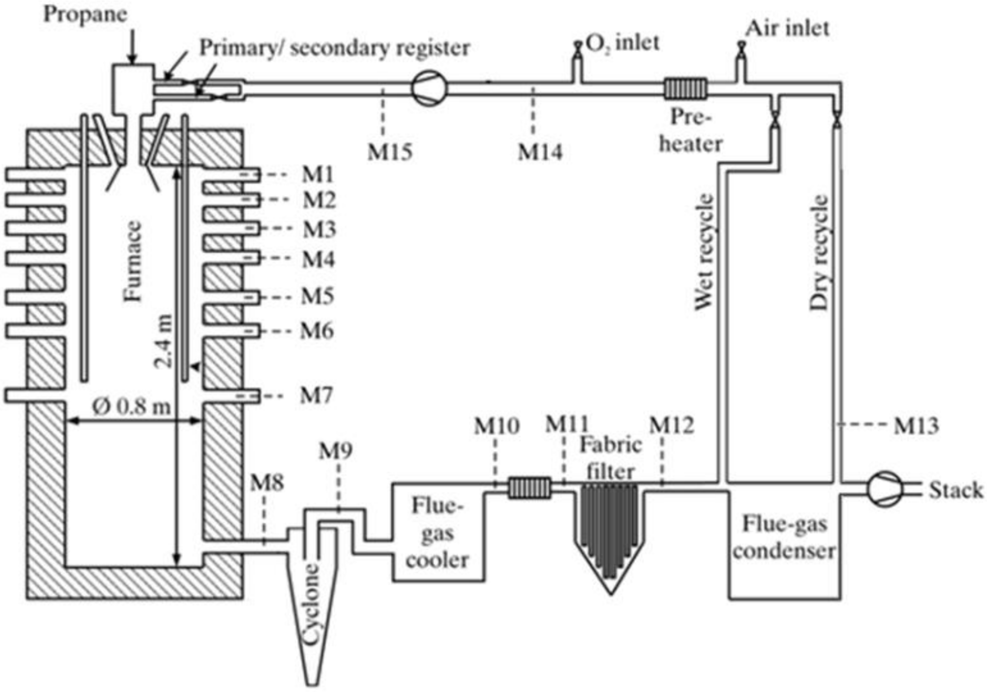

Figure 4.1 Schematic of the Chalmers 100 kW oxy-fuel test rig. The measurements were performed in measurement ports M2 – M5 in this work.

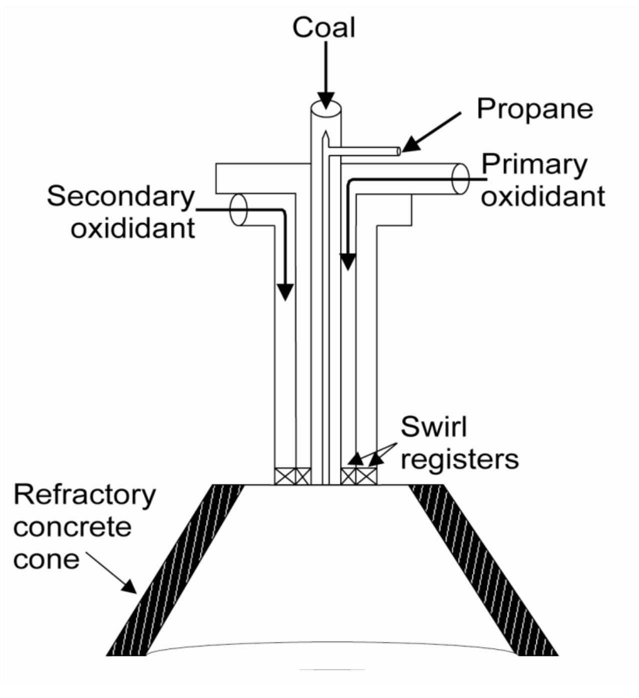

Figure 4.2 Configuration of the lignite burner

4.2 Experimental Combustion Furnace (ECF)

The Experimental Combustion Furnace (ECF) is a 400 kW_{fuel} scale model of LKAB's rotary kiln furnaces in Kiruna, Fig 4.3. The ECF is scaled to mimic the combustion conditions in the kiln in the full scale process plants. The furnace is 14 m long and the inner diameter is 0.8 m. The combustion conditions are significantly different from the conditions in the Chalmers unit, since a very high air-to-fuel ratio is used, and as the air is preheated to a high temperature. The burner is mounted in the centre of the furnace, and above and below the burner there are two large ducts where the main part of the air is supplied, Fig 4.2. The air is preheated to 1100°C to resemble the temperature of the air from the cooler in the real plants. The air is supplied through a honey comb structure in the ducts to create a homogenous flow field. The total flow of air is around 2200 Nm^3, which results in an O_2 concentration in the exhaust of 17-18%. The furnace is equipped with a number of measurement ports along the length of the furnace. In this work the first five ports were used since flame measurements were of interest. Quartz windows were placed on the opposite side of port 2-5, which were used as cold backgrounds in the radiation intensity measurements. Several different fuels including gas, oil and solid fuels can be used in this facility with different burners designed for the specific fuels.

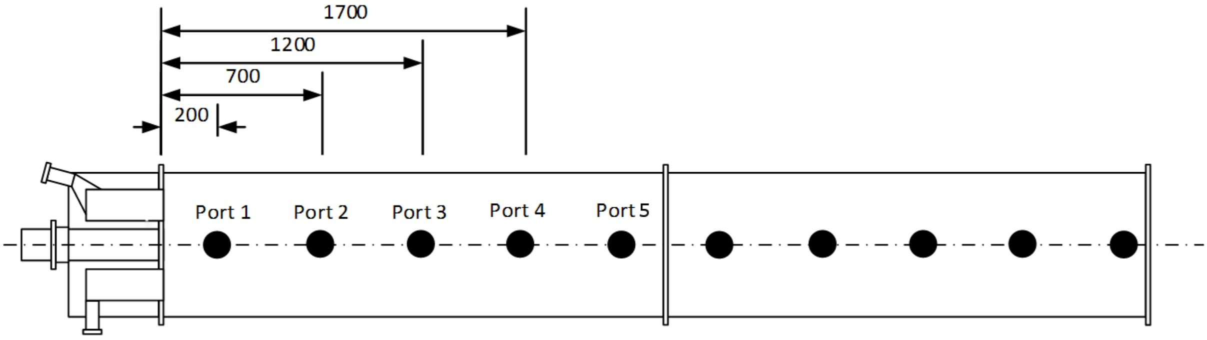

a)

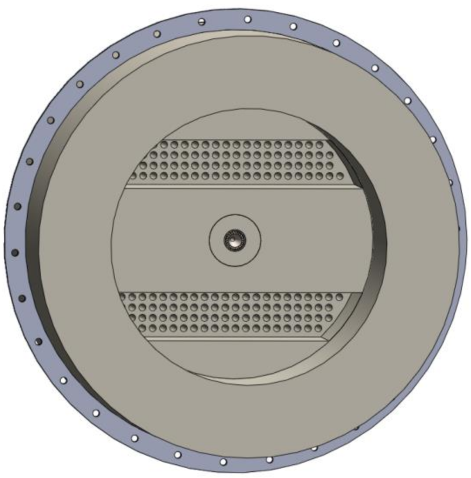

b)

Figure 4.3 a) First part of the ECF showing the measurement ports used. **b)** Cross-section of the furnace showing the central burner and air ducts above and below the burner.

4.3 Measurement techniques applied in this work

As one of the aims with this work was to evaluate and find suitable measurement techniques for quantification of particle radiation in flames, several different techniques have been tested. The selection of the tested measurement techniques were made based on the potential for adding new information needed for the understanding of the particle radiation, but also on their availability. By co-operation with other research groups at Chalmers and other Universities it was possible to evaluate several advanced measurement techniques (optical FTIR, SMPS, PASS-3, DLPI) in this work without the time consuming and expensive procedure of purchasing the equipment. Out of the measurement techniques presented in Chapter 3, the following methods have been used in this work:

- Narrow Angle Radiometer (Paper I-V)
- Ellipsoidal element (Not published)
- Suction pyrometer (Paper I-V)
- FTIR (Paper I and IV)
  - Gas analysis
  - Optical measurements
- Particle extraction system (Paper II, III and V)
  - SMPS
  - Low Pressure Impactor
  - Cyclone
  - Sintered brass filter
  - PASS-3

5. Radiation modelling

Radiation modelling has been used in this work to analyse the information gained from the various techniques used for in-flame measurements. The following chapter describes the modelling approach used in this work. Modelling of radiation in a combustion chamber is a complicated task due to the variations in temperature, gas concentration, particle concentration and particle type in a combustion chamber, but also due to the spectral dependence of the radiative properties of the gases and particles. A radiation model needs to account for the directional variations of the intensity, and also needs sub-models to account for the radiative properties of the medium, which in combustion environments with their large spectral variations becomes computationally demanding. The modelling approach applied in this work is used to study the influence on the flame radiation from different parameters, such as different types of particles, gases and their temperature, to address the research questions in Chapter 1.4. Therefore, detailed models are applied for calculation of the gas and particle properties, but the investigated geometry is kept relatively uncomplicated. The modelling and radiative property models used in this work is summarized in this section, more details can be found in Paper I-V.

5.1 Gas radiation

The transmissivity of the gas is a function of the temperature and concentration of the absorbing gas species, mainly CO_2 and H_2O. The model used in this work is the Malkmus Statistical Narrow Band model [84], with a spectral resolution, i.e. bandwidth, of 25 cm^{-1}, which means that several hundreds of bands are needed for the spectrum of interest. The transmissivity, $\bar{\tau}_k$, of each narrow band is calculated according to Eq. (5.1). The overbar indicates that it is a spectral average for the band.

$$\bar{\tau}_k = \exp\left[-\frac{2\gamma}{d_k}\left(\sqrt{1+\frac{YPLk_kd_k}{\gamma}}-1\right)\right] \tag{5.1}$$

Where Y is the mole fraction of the absorbing species, P is the total pressure and L is a characteristic length. The parameters k_k and d_k are temperature dependent parameters for each gas, and are taken from the work of Rivière and Soufiani [85]. The half-widths, γ, of the absorbing species are calculated from Eq. (5.2) and (5.3) with P_s =1 bar and T_s = 296 K.

$$\gamma_{CO_2} = \frac{P}{P_s}\left(\frac{T_s}{T}\right)^{0.7}\left[0.07Y_{H_2O} + 0.058\left(1 - Y_{CO_2} - Y_{H_2O}\right) + 0.1Y_{H_2O}\right] \tag{5.2}$$

$$\gamma_{H_2O} = \frac{P}{P_s}\left\{0.462Y_{H_2O}\left(\frac{T_s}{T}\right) + \left(\frac{T_s}{T}\right)^{0.5}\left[0.079\left(1 - Y_{CO_2} - Y_{O_2}\right) + 0.106Y_{CO_2} + 0.036Y_{O_2}\right]\right\} \tag{5.3}$$

To account for non-uniform paths the Curtis–Godson approximation is applied [86] and the total transmissivity ($\bar{\tau}_{k,g}$) of the gas mixture is calculated as the product of the transmissivity of the absorbing gases, Eq. (5.4)

$$\bar{\tau}_{k,g} = \bar{\tau}_{k,H_2O}\,\bar{\tau}_{k,CO_2} \tag{5.4}$$

5.2 Particle radiation

The governing parameters for the particle properties, *i.e.* absorption and scattering efficiency, Q_{abs} and Q_{scat}, can be calculated with the Mie-theory as a function of the size parameter, *x*, and the complex index of refraction, *m*.

$$x = 2\pi r_p/\lambda \tag{5.5}$$

$$m = n - ik \tag{5.6}$$

The size parameter relates the particle radius, r_p, to the wavelength of the radiation, Eq. (5.5). The complex index of refraction is a material specific parameter determining how much of the radiation that is absorbed and scattered, Eq. (5.6). In contrast to the radiative properties of the gas, there are larger uncertainties of the complex index of refraction of the particles. There are significant differences in literature data on the complex index of refraction, especially for ash particles. The determination of the particle size distribution, and thereby also the size factor, and the particle types present in a flame is also challenging. The properties between the particle types varies significantly and the particle size have a large influence on the radiative properties when the size parameter is around unity, which for combustion temperatures means diameters of a few microns.

Unburned fuel particles and the residual char particles can be assumed to have the same radiative properties. Different complex refractive indices were tested in Ref. [45] for these particles and the results showed only a minor influence on the results due to the fact that these particles typically have a size in the range of tens of µm. The complex index of refraction used in this work is taken from Ref. [76], other examples of available data are presented in Refs. [87, 88]. The refractive indices for ash particles from Refs. [77-79] are used in this work as implemented in Ref. [47]. Also for soot there are several differences in the reported data of the complex index of refraction. The results from Chang and Charalampopoulos [75] are mainly used in this work, but other correlations [72-74] have also been tested.

For small non-scattering particles, such as primary soot particles, the absorption coefficient can be calculated based on the Rayleigh theory. The absorption coefficient of a cloud of soot particles is then not dependent on the particle size, but only on the soot volume fraction and the complex index of refraction, [48].

$$\kappa_\lambda = \frac{36\pi nk}{(n^2-k^2+2)^2+4n^2k^2}\frac{f_v}{\lambda} \tag{5.7}$$

5.3 Solution of the RTE

The discrete transfer method [89] has been used to calculate the intensity field. In this method the RTE is solved for rays along specific directions, and the radiative flux is given by a weighted summation of these rays. To determine the intensity along a ray the correlated formulation of the RTE, accounting for a difference in temperature between the gas and particles was used to calculate the intensity in each spectral band, Eq. (5.8). The summation in the equation corresponds to the discretization of the path shown in Fig. 5.1. The scattering by particles is assumed to be isotropic and particle properties are calculated for each narrow band. Ash and coal particles are assumed to have the same temperature, whereas the soot is assumed to have the same temperature as the gas. In this case, the absorption coefficient of the soot is added to the absorption coefficient of the gas, while the char and ash coefficients are summed together. The total intensity is finally obtained by a summation of the intensity of all bands. Details on the derivation of Eq. (5.7) are given in Paper I.

$$\begin{aligned}\bar{I}_{\upsilon_k,n} = {} & \bar{I}_{\upsilon_k,0}\bar{\tau}_{\upsilon_k,0\to n} \\ & + \sum_i \Big(\big(1-\bar{\omega}_{\upsilon_k,i+1/2}-\bar{\psi}_{\upsilon_k,i+1/2}\big)\bar{I}_{b\upsilon_k,i+1/2}(T_g) + \bar{\psi}_{\upsilon_k,i+1/2}\bar{I}_{b\upsilon_k,i+1/2}(T_p) \\ & + \bar{\omega}_{\upsilon_k,i+1/2}G_{scat,i+1/2}\Big)\big(\bar{\tau}_{\upsilon_k,i+1\to n}-\bar{\tau}_{\upsilon_k,i\to n}\big)\end{aligned} \tag{5.8}$$

$$\bar{\psi}_{\nu_k} = \frac{\kappa_{\upsilon_k,coal}+\kappa_{\upsilon_k,ash}}{\beta_{\upsilon_k,coal}+\beta_{\upsilon_k,ash}-\ln\left(\bar{\tau}_{\upsilon_k,g}\right)/\Delta s} \tag{5.9}$$

The parameter $\bar{\psi}_{\nu_k}$, is introduced to account for the difference in particle and gas temperatures, while $\bar{\omega}_{\upsilon_k}$ is the scattering albedo which relates the amount of scattering to the total extinction coefficient.

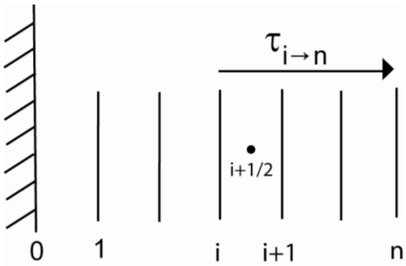

Figure 5.1. Discretization of a pathway.

5.4 Indirect determination of the particle radiation

The expected accuracy of the gas radiation modelling is high, assuming that the gas temperature and concentration is measured correctly. The total radiative intensity measured with the narrow angle radiometer also has a high accuracy. Figure 5.2 shows an example of a measured intensity profile in port 4 in the ECF. The measured intensity is a result of the emitted and scattered radiation of the gas and particles along the path from the probe to the window. The gas radiation is calculated for the same path as the intensity is measured using the measured gas temperature and concentration as input. As the figure shows, there is a gap between the modelled gas radiation and measured total intensity. The shaded area corresponds to the particle radiation. So, without any further modelling it is possible to predict the contribution from particle radiation. However, the source of the particle radiation is then unknown and depending on the fuel, the source is radiation from soot, fuel/char or ash particles (or all three types). In the work presented in this thesis, different measurement techniques are combined with radiation modelling to describe the source of the particle radiation, *i.e.* separate between the particle types present in the flame.

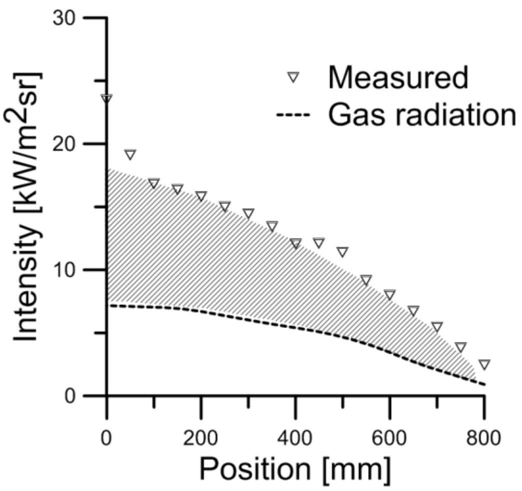

Figure 5.2. Measured radiative intensity profile and modelled gas radiation. The shaded area is a result from the contribution by particle radiation.

6. Results and discussion

6.1 Combustion conditions

Various combustion conditions have been investigated in the work presented in this thesis. The aim has been to examine the radiative heat transfer, with particular focus on the particle radiation in flames. The main attention is put on conditions relevant for pilot or large scale combustion, *i.e.* combustion of pulverized fuels in relatively large flames. Results from the two units are included, primarily the 100 kW test rig at Chalmers, but also from the 400kW$_{fuel}$ ECF. The Chalmers test unit offers great possibilities of changing the combustion conditions by allowing recycling of flue gases and feeding of pure oxygen. By recirculating different amounts of flue gas, the oxygen concentration can be changed, and thereby the flame temperature and soot formation conditions may be altered drastically. The test unit also allows the use of both solid and gaseous fuels, and the studies presented here include experiments on propane and lignite. The propane flames show examples of how the influence of soot radiation can be isolated and studied in detail, while the lignite flames include also fuel, char and ash particles in addition to soot particles.

The photos in Fig. 6.1 and 6.2 show examples of flames in which the radiative heat transfer has been investigated. Figure 6.1a –d shows photos of different propane fired flames in the Chalmers test unit taken through the quartz window in port M2. The refractory burner quarl can be seen in the top of the photos and the measurement port on the opposite side is seen in the background of Figure 6.1 b. The cases shown are: a) air firing b) oxy-fuel with 25 vol % O_2 in the oxidizer (OF25), c) OF30 and in d) OF36. The color of the flame varies from blue to yellow, where the blue color is a result of chemiluminescence emitted by radicals, while the yellow colour is caused by emission from hot soot particles. As the photos show the amount of soot varies between the cases where the OF25 flame is non-sooting, and the OF36 flame contains a significant amount of soot. The blue flame serves as a good reference for how gas radiation is accounted for in the modelling, since the particle radiation can be neglected in this case (this has also been confirmed by soot particle measurements in Paper III). Figure 6.1 e) shows an air fired lignite flame in port M2 and the flames shown in f) – h) are propane and lignite in port M3. The probe shown in the photos is the optical probe used in the FTIR based measurements presented in paper I and IV.

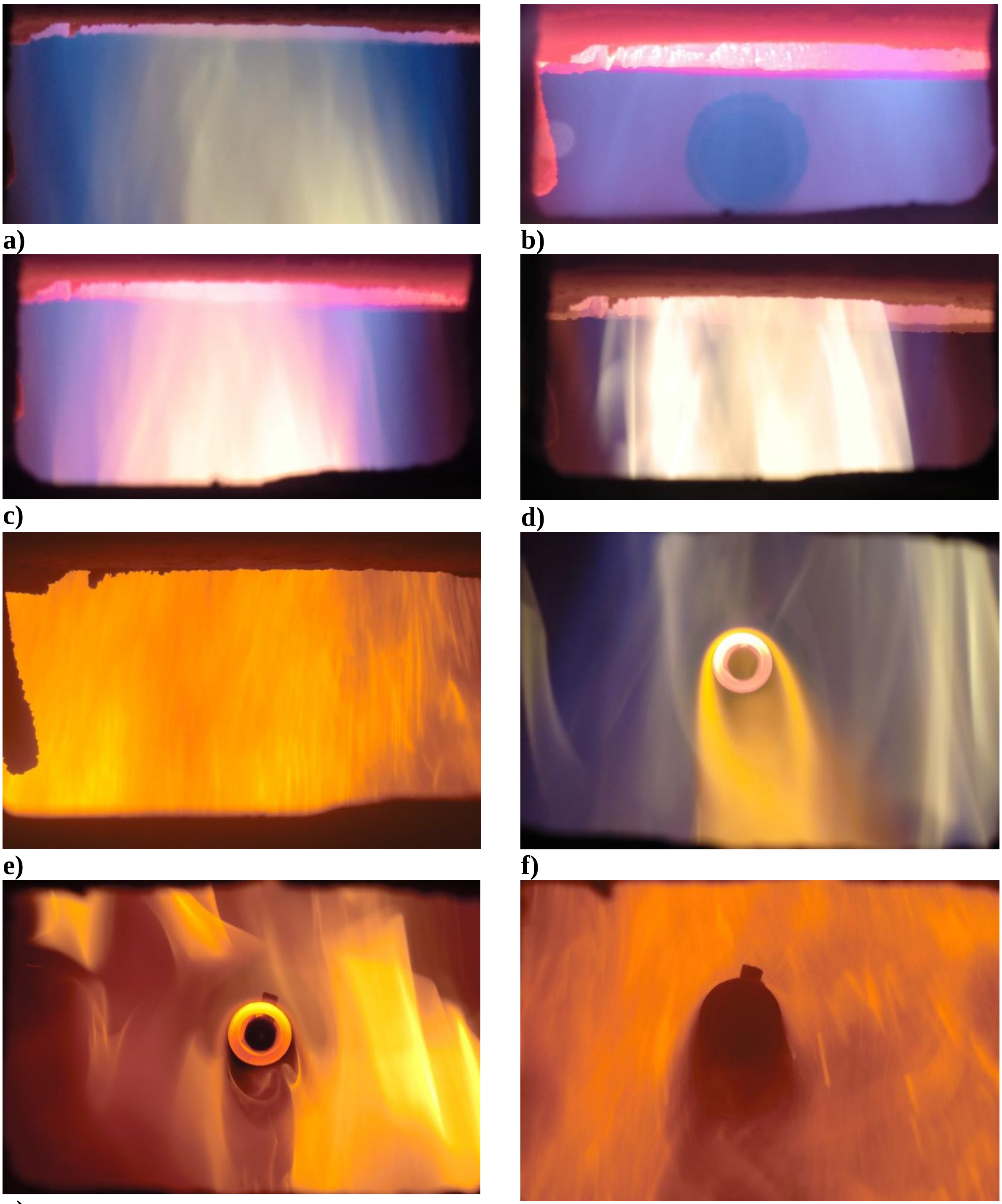

Figure 6.1. Examples of flames studied in the Chalmers test unit. Photos are taken in Port M2 for **a)** air-propane, **b)** OF25-propane, **c)** OF30-propane, **d)** OF36-propane and **e)** air-lignite. The optical probe used in the FTIR measurements is shown in port M3 in panels **f)** – **h)**. The test cases are: **f)** air-propane, **g)** OF36-propane and **f)** air-lignite.

Figure 6.2 shows examples of the conditions in the ECF experiments, with a) and b) showing the burner and c) and d) a position further downstream. The test case in Fig. 6.2a is a pre-mixed co-firing flame with 70% coal and 30% biomass treated with steam explosion, Fig. 6.2b shows a flame with 10% of the same biomass as in a) but with coal and biomass fed in separate registers of the flame resulting in a broader flame with faster ignition of the fuel.

Figs. 6.2c and d show examples of a natural gas flame and a coal flame respectively. As seen, the length of the flame is highly dependent on both the burner geometry and the fuel, as anticipated. The gas flame only extends to port 2, while a significant amount of unburned particles can be observed this position in the solid fuel flame. The intensity probe is visible in the measurement port on the opposite side of the furnace.

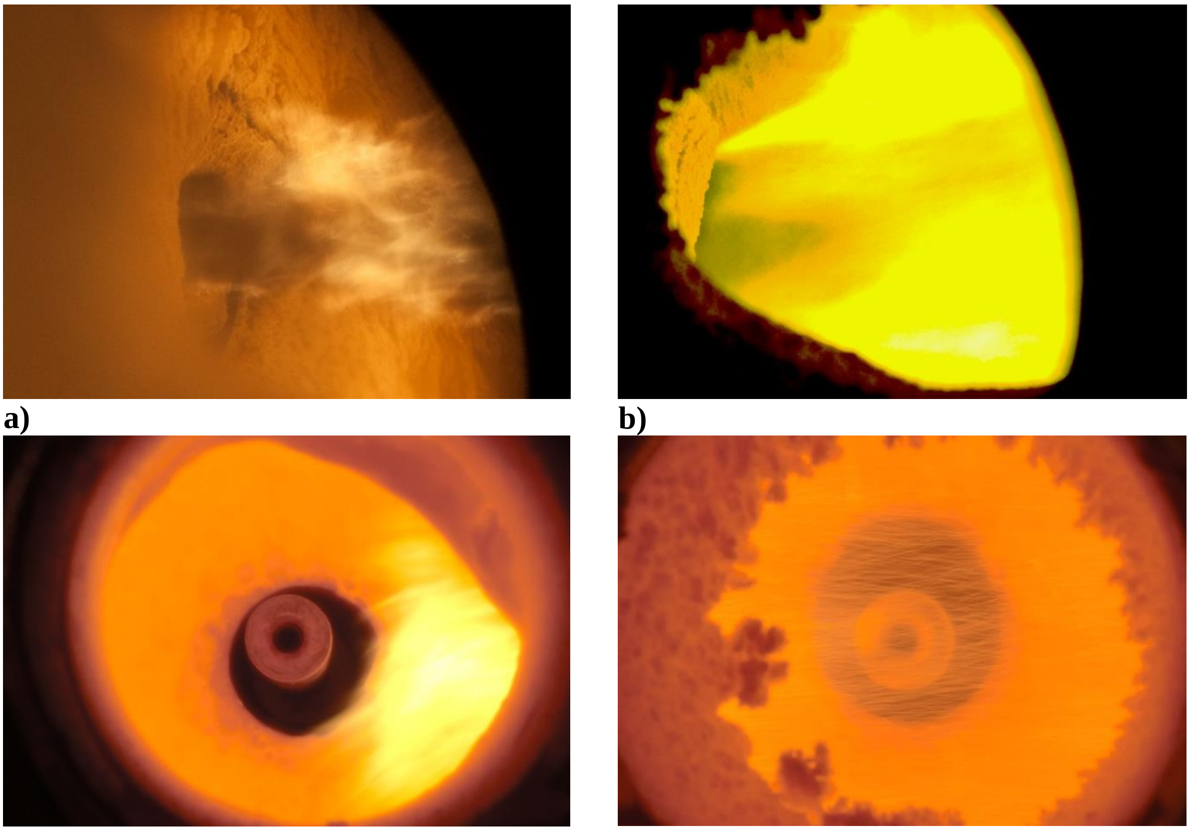

a) **b)** **c)** **d)**

Figure 6.2. Examples of flames studied in the ECF. The first port where the burner can be seen is shown in **a)** and **b)** with two co-firing flames using different burners. **c)** and **d)** shows conditions in port 2 for natural gas and coal respectively (the intensity probe can be seen in the background).

6.2 Particle temperature

Particle temperature is one of the most important parameters for understanding radiation emitted by a flame. Paper I is focused on the measurement of spectral radiation in an air fired lignite flame in Chalmers 100 kW test facility. Figure 6.3 a) shows the cross-section of the Chalmers furnace where the measurements were performed, the measurement points are indicated with dots and the bars represent the optical path length of the 15 cm long measurement volume. The path length of 15 cm was chosen to obtain a high emissivity of CO_2 in the region around 2350 cm^{-1}, thus enabling gas temperature measurements. The measured spectral radiation is the result of emission from particles and gases in the measurement volume. From the measured spectrum it is possible to estimate the particle concentration and temperature as described in Section 3. Figure 6.3 b) shows the resulting particle temperature profile, and the temperature profile measured with the suction pyrometer is also included in the figure. The particle temperature in this position of the flame was found to be lower than the gas temperature. It is important to note that the temperature measured with the optical technique is an average over the 15 cm long path. If these particle temperature measurements were to be repeated, it is recommended to decrease the distance as much as possible with consideration to the signal strength, to obtain a better spatial resolution. By analyzing the spectrum it was possible to conclude that the particle radiation to a large extent was caused by coal/char particles. The temperature profile should therefore be interpreted as the coal/char temperature. The soot particles are more likely to have the same temperature as the gas, and it was also concluded that the volume fraction of the soot is likely less than 1E-7.

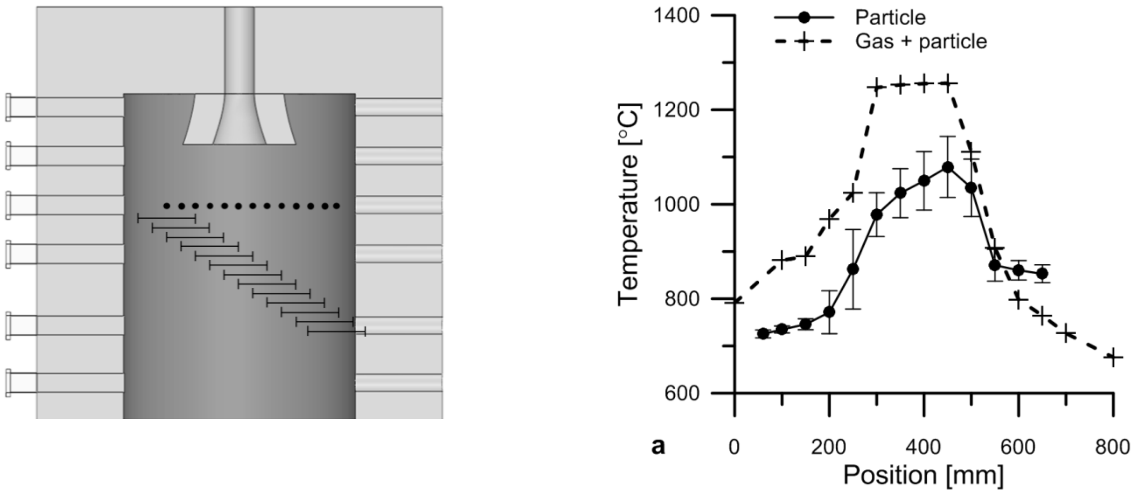

Figure 6.3. a) Measurement positions and optical paths used for the optical probe measurements in the Chalmers test unit. **b)** Temperature profiles using the FTIR technique for particle temperature and suction pyrometer for the gas and particle temperature.

Radiation modelling, using the results from the optical measurements, showed good agreement with the measured intensity, Fig. 6.4a, which indicate that the estimated particle temperature is quite accurate in this position of the flame. The estimated accuracy of the fitting procedure is +/- 50K, and the influence from such changes in particle temperature is shown in Fig. 6.4b. The modelling further stresses that particle radiation is the main contributor to the total radiation in this cross-section of the flame.

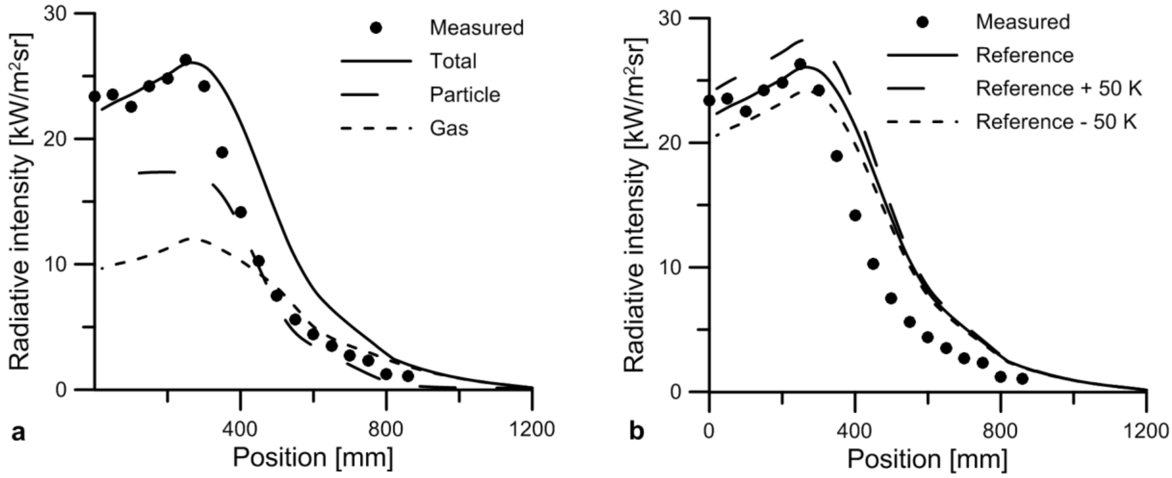

Figure 6.4. a) Modelled and measured radiative intensity in the Chalmers test unit. **b)** Sensitivity analysis of particle temperature.

6.3 Particle types

It was recognized during the measurements with the optical techniques that additional knowledge of the particle type and size would increase the accuracy of the particle radiation modelling due to the varying spectral radiative properties of the different particle types. Extractive particle measurements using a low-pressure impactor (DLPI) were therefore used to characterize the particles in the center of the same lignite fired flame, and the results are presented in paper II. The aim was to add information to further test and to confirm the results found in paper I. Particles larger than 10 µm were collected in a cyclone and particles between 30 nm and 10 µm were separated into 13 stages in the DLPI. The size distribution by mass is obtained from the measurement and it was found that a significant amount of the mass could be found in the cyclone. Two stages in the DLPI were analyzed with SEM-EDX to clarify what type of particles that was present in the flame. The particles collected on the 50 nm stage were concluded to be primary soot particles due to their high carbon content. These particles appeared visually in the microscope to be spherical and had a diameter close to the expected size of primary soot particles, Fig 6.5b. The particles on the 2.9 µm stage were a mix of fuel/char (C), fuel/ash particles (B) and pure ash particles (A), Fig. 6.5a. The particles in the cyclone were not investigated in a microscope, but their black color indicated that the main part of the sample was fuel/char particles. The size distribution of the cyclone particles were investigated with laser diffraction and an average diameter of these particles were found to be 24 µm in this case.

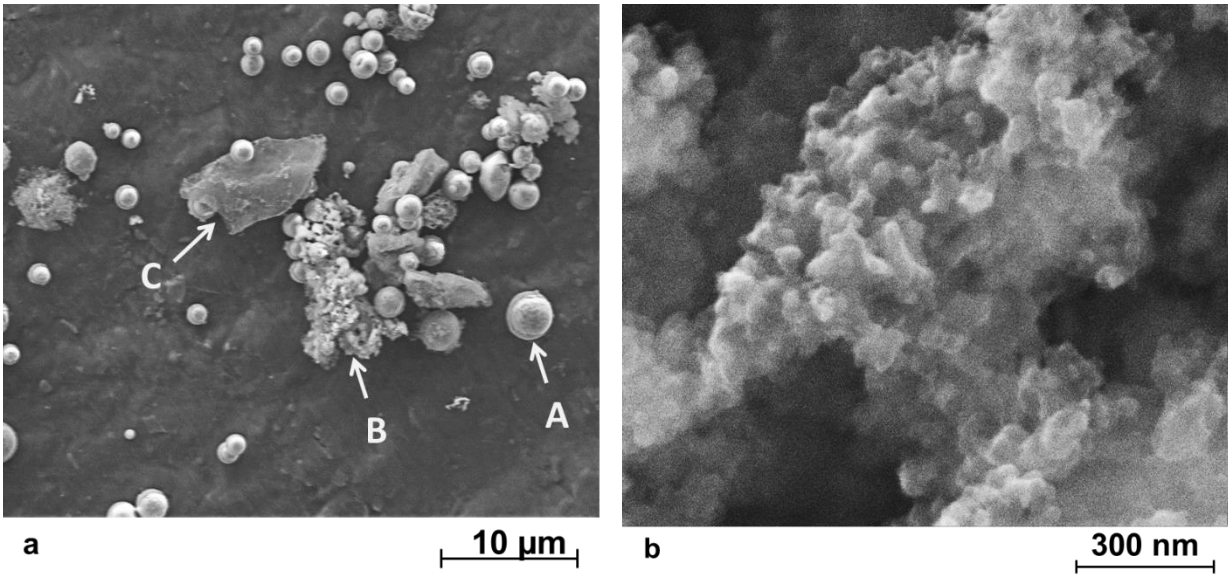

Figure 6.5. SEM-images of particles collected in the centre of the Lignite flame in the Chalmers unit on a) stage 10 (2.9 µm) and b) stage 2 (50 nm) in the DLPI.

The radiative intensity was calculated using the measured concentrations of soot, ash and char particles. Particles smaller than 180 nm (stage 1-4 in the DLPI) were assumed to be soot particles and the intermediate particles (stage 5-13) were assumed to be ash and the cyclone particles were modelled as coal/char particles. The different size fractions were treated separately in the modelling and thereby providing a possibility to study the influence of different size fractions. The results from such an analysis are shown in Fig. 6.6. Gas radiation was first modelled separately and then one particle size group was added at a time starting with the smallest particles. As seen, the lower lines are closely spaced indicating only a small influence on the radiative heat transfer from these particle sizes. However, the top line, which represents the cyclone particles, is significantly above the others and this shows the important contribution of the char particles collected in the cyclone. This corresponds well with the results presented in Paper I where it was seen that smaller soot particles have a moderate influence in the investigated flame. The agreement between measured and modelled intensity is not as good in this case as in Fig. 6.4. A sensitivity analysis was performed, which indicated that a too low particle temperature and the dilution factor in the probe are two factors which likely may explain the difference in the results.

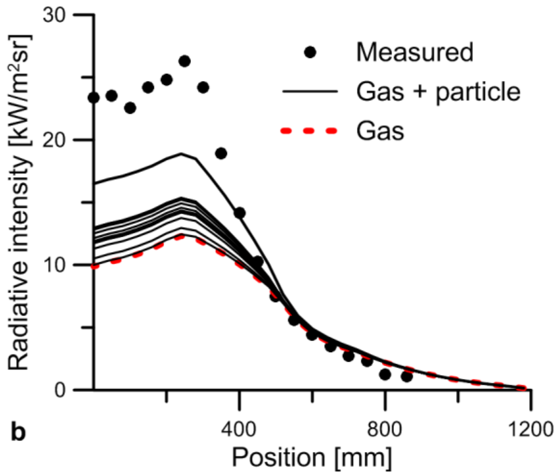

Figure 6.6. Measured and modelled radiative intensity in the investigated cross-section of the lignite flame in the Chalmers unit, with the DLPI stages modelled as ash and soot particles and the cyclone particles as char. The solid lines correspond to the DLPI stages and the cyclone, with the lowest line including only stage 1 and then adding one stage per line.

The particle extraction system was refined after the conduction of the experimental campaigns presented above and a new probe and dilution system were designed. Compared to the system used for the measurements in the lignite flame (Paper II) the main improvements are: oil-cooling of the probe to enable higher temperatures in the probe, addition of nitrogen with calibrated mass flow controllers, and, that all flows are measured with flow-meters. Experiments with propane was selected for a test of this setup due to the possibilities of creating better defined combustion conditions in a propane flame compared to a lignite flame. The particle size distribution was in this measurement campaign measured with the SMPS instrument and the results are presented in Paper III. Two different air-fired flames were investigated, one sooting and one non-sooting. The soot formation was increased by modifying the distribution of air in the burner. Figure 6.7a shows the intensity profile in the flame with a low soot volume fraction. The black solid line is modelled gas radiation using the measured gas concentrations and temperature as input. The soot volume fraction was $>10^{-9}$ in this flame and the contribution from soot is thus negligible. The agreement between the modelled intensity and the measured data, grey dots, is good showing that the gas radiation is well predicted with the modelling approach applied. Figure 6.7b shows the measured and modelled intensity in the sooting flame, where the soot volume fraction measured with the SMPS, 6E-8, was used as input to the model. The modelled total intensity agreed well with the measured intensity for these conditions, indicating that the measured soot volume fraction is accurate. The intensity measured with the narrow angle radiometer was similar in both flames, but the temperature in the sooting flame was approximately 100°C lower.

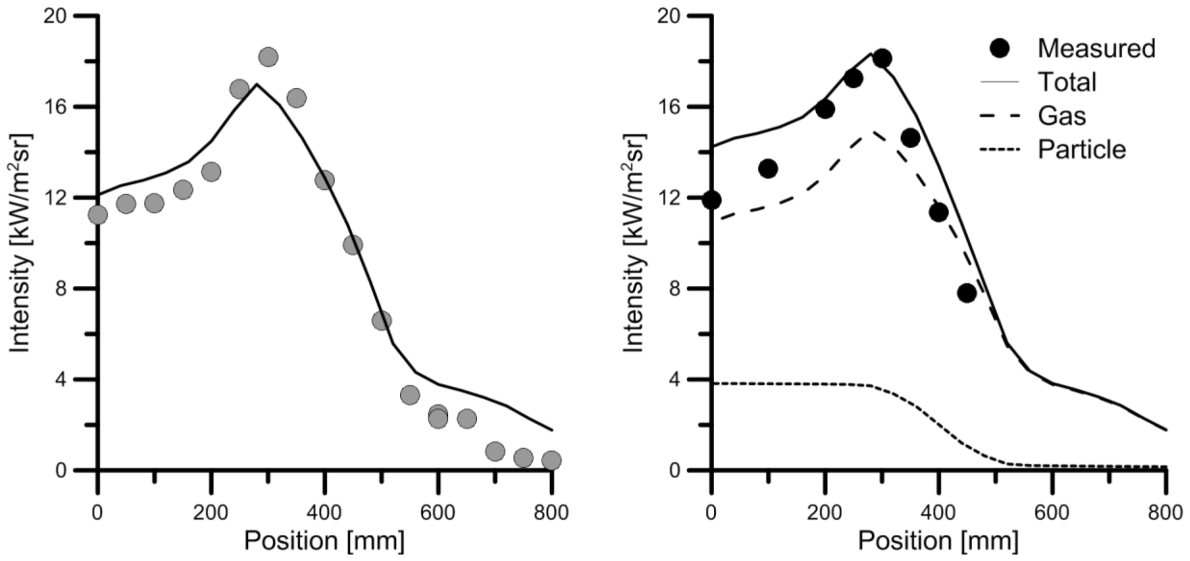

a) **b)**

Figure 6.7. Radiative intensity profiles for two air-fired propane flames in the Chalmers unit: **a)** non-sooting, **b)** sooting. The modelled gas, particle and total radiation is also shown.

6.4 Flame radiation from different fuels

The work presented in Paper V focuses on the influence of different fuels on the radiative heat transfer in rotary kiln applications. Due to the high air excess used in the ECF, the contribution of gas radiation was low and the particle radiation was found to dominate the radiation. When evaluating the fuels it is the two previously discussed parameters that differs, particle/flame temperature and amount and type of particles. The presence of different types of particles including the propensity for soot formation are most important properties of the fuel when predicting radiative heat transfer from a flame. The measurement conditions in the ECF were challenging with very high flame temperatures, and it was therefore not possible to obtain reliable temperature or particle data from the flame. The evaluation of the heat transfer and influence of the fuels was instead mainly based on the measured radiative intensity. Some of the most interesting results found, which pinpoints the importance of the topic of this thesis is shown in Fig. 6.8. This figure shows the measured radiative intensity in three ports of the ECF for two different coals. The coals are very similar both with respect to size distribution and proximate and ultimate analysis. Despite the similar fuel specifications, the resulting radiative intensity is significantly higher for one of the coals (Coal B). This shows the difficulties of predicting the radiative heat transfer from a flame when *e.g.* changing fuel, even though seemingly small changes in the fuel composition are made. In this case, the explanation is believed to be a faster fragmentation of Coal B than Coal A, thereby creating smaller char particles and a larger projected surface area in the flame. An increased soot formation can also explain the difference, but considering the similarity of the fuels and knowledge that it is mainly the amount of tar in the fuel that governs the soot formation [25], it is not likely that the soot formation differs significantly between these two fuels.

Further conclusions from this work (Paper V) show that it is possible to obtain similar peak values of the radiative intensity in co-firing flames with 10 and 30% biomass as in coal flames. But, the radiative length of the co-firing flames were shorter *i.e.* the intensity in the post flame zone was lower than for the coal flames. This is likely caused by the coarser biomass particles resulting in lower particle temperature and lower projected surface area per mass of fuel.

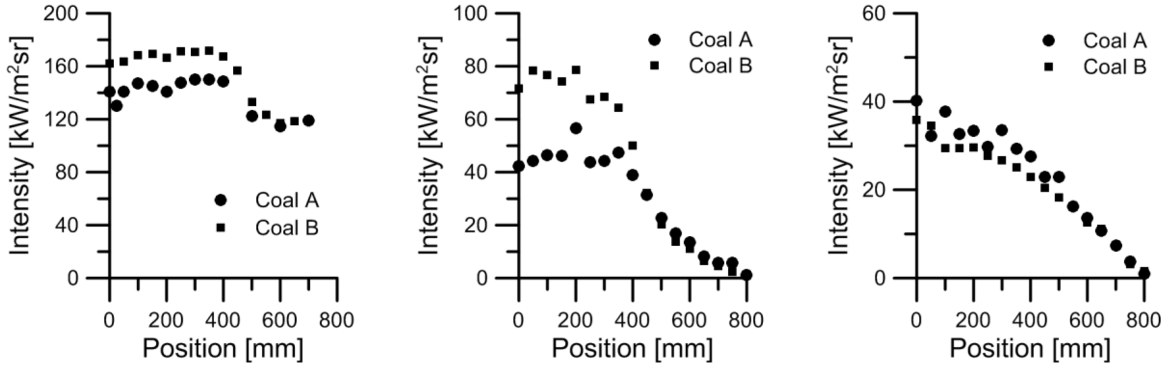

a) **b)** **c)**

Figure 6.8. Measured radiative intensity profiles in the ECF for Coal A and Coal B in **a)** Port 1, **b)** Port 2 and in **c)** Port 4.

7. Conclusions

The work presented in this thesis aims to develop a methodology for the quantification of particle radiation in flames and to show the influence from important parameters such as particle temperature, particle size distribution and particle type. This has been done by combining measurements with detailed radiation modelling to address the influence from particle radiation on the total radiative heat transfer. The experimental work was performed in the Chalmers 100 kW oxy-fuel test unit and in a 400 kW scale model of a rotary kiln furnace. Measurements of radiation intensity using a narrow angle radiometer serve as reference in all studies since it provides a good measure of the flame radiation without influence from walls or other surfaces. The in-flame particle temperature and concentration were measured with an FTIR based system. A particle extraction system has also been developed where the particle type, size distribution and optical properties have been analyzed with a low pressure impactor, scanning mobility particle sizer and a photo acoustic soot spectrometer. Detailed descriptions of the particle properties with the Mie-theory and a statistical narrow band model are used in the radiation model. The methodology, in which measurements are combined with modelling, shows good possibilities of quantifying the particle radiation in flames. The influence of particle type, size distribution and temperature has also been shown in the modeling. In all investigated solid fuel flames particle radiation dominated the total radiation. In the investigated lignite flame in Chalmers 100 kW test unit, char particles give the largest contribution to the particle radiation whereas the soot only has a minor influence in this position of the flame. From the spectral analysis of the particle radiation, the temperature of the char particles was found to be 200°C lower than the gas temperature. The soot volume fraction measured with the SMPS instrument in an air fired propane flame represent particle radiation corresponding well with the expected particle radiation, *i.e.* the difference between modelled gas radiation and measured total radiation. Results from the 400 kW study show that it is possible to obtain similar radiation intensity in the co-firing flames as in the coal flames. Radiation measurements in flames of two almost identical coal types under similar combustion conditions revealed a significant difference in the radiative intensity. This result shows the difficulty of predicting flame radiation without performing measurements, since the radiation depends on factors such as soot formation, which is highly dependent on fuel and combustion conditions.

8. Suggestions for Future Work

A large part of this work has been to develop a methodology for characterization of particles and particle radiation in flames. The main intention with the presented results has been to demonstrate the possibilities using the methodology developed in this work. It should therefore be of interest to increase the test matrix in terms of other fuels and combustion conditions to draw more general conclusions. The following areas should be of particular interest:

- The role of soot radiation in coal flames is a topic where further research is needed, especially with respect to measurements within the flames in which all particle types are present to show the influence from char, soot and ash particles on the radiative heat transfer conditions. This may be done in experiments using the FTIR based technique and extractive particle measurements, in combination with the radiation model.

- A comparison with particle temperature measurements using both two-color pyrometry in the visible spectral region and FTIR in a flame with both char and soot particles would be of interest. The increased absorption by soot particles in the visible spectral region can cause problems to separate these two techniques. By using spectral models for the properties of char and soot particles it may be possible to separate between the char and the soot temperature by analyzing both the IR and visible spectrum. Comparisons of particle temperature techniques in flames of technical scale have not been found in the literature and would be valuable for future works on flame radiation.

- The photo acoustic soot spectrometer has only been used in a short measurement campaign in this work. However, the instrument provides interesting results and it would be highly interesting to investigate if and how this instrument works with coal/char particles. Using this instrument for measurements in a coal flame can be a valuable tool for evaluation of complex index of refraction of particles in a coal flame.

9. Bibliography

1. IEA, *World Energy Outlook 2012*. 2012, OECD Publishing.
2. Toftegaard, M.B., J. Brix, P.A. Jensen, P. Glarborg, and A.D. Jensen, *Oxy-fuel combustion of solid fuels.* Progress in Energy and Combustion Science, 2010. **36**(5): p. 581-625.
3. Williams, A., M. Pourkashanian, and J.M. Jones, *Combustion of pulverised coal and biomass.* Progress in Energy and Combustion Science, 2001. **27**(6): p. 587-610.
4. Wall, T., Y. Liu, C. Spero, L. Elliott, S. Khare, R. Rathnam, F. Zeenathal, B. Moghtaderi, B. Buhre, C. Sheng, R. Gupta, T. Yamada, K. Makino, and J. Yu, *An overview on oxyfuel coal combustion-State of the art research and technology development.* Chemical Engineering Research and Design, 2009. **87**(8): p. 1003-1016.
5. Jordal, K., M. Anheden, J. Yan, and L. Strömberg, *Oxyfuel combustion for coal-fired power generation with CO2 capture—Opportunities and challenges*, in *Greenhouse Gas Control Technologies 7*, E.S.R.W.K.F.G. Wilson and T.M.G. Thambimuthu, Editors. 2005, Elsevier Science Ltd: Oxford. p. 201-209.
6. Jonsson, C.Y.C., J. Stjernberg, H. Wiinikka, B. Lindblom, D. Boström, and M. Öhman, *Deposit Formation in a Grate-Kiln Plant for Iron-Ore Pellet Production. Part 1: Characterization of Process Gas Particles.* Energy & Fuels, 2013. **27**(10): p. 6159-6170.
7. Viskanta, R. and M.P. Mengüç, *Radiation heat transfer in combustion systems.* Progress in Energy and Combustion Science, 1987. **13**(2): p. 97-160.
8. Tien, C.L. and S.C. Lee, *Flame radiation.* Progress in Energy and Combustion Science, 1982. **8**(1): p. 41-59.
9. Scheffknecht, G., L. Al-Makhadmeh, U. Schnell, and J. Maier, *Oxy-fuel coal combustion—A review of the current state-of-the-art.* International Journal of Greenhouse Gas Control, 2011. **5, Supplement 1**(0): p. S16-S35.
10. Molina, A. and C.R. Shaddix, *Ignition and devolatilization of pulverized bituminous coal particles during oxygen/carbon dioxide coal combustion.* Proceedings of the Combustion Institute, 2007. **31 II**: p. 1905-1912.
11. Shaddix, C.R. and A. Molina, *Particle imaging of ignition and devolatilization of pulverized coal during oxy-fuel combustion.* Proceedings of the Combustion Institute, 2009. **32 II**: p. 2091-2098.
12. Ayling, A.B. and I.W. Smith, *Measured temperatures of burning pulverized-fuel particles, and the nature of the primary reaction product.* Combustion and Flame, 1972. **18**(2): p. 173-184.
13. Solomon, P.R., P.L. Chien, R.M. Carangelo, P.E. Best, and J.R. Markham, *Application of FT-IR emission/transmission (E/T) spectroscopy to study coal combustion phenomena.* Symposium (International) on Combustion, 1989. **22**(1): p. 211-221.
14. Solomon, P.R., R.M. Carangelo, P.E. Best, J.R. Markham, and D.G. Hamblen, *Analysis of particle emittance, composition, size and temperature by FT-i.r. emission/transmission spectroscopy.* Fuel, 1987. **66**(7): p. 897-908.
15. Khatami, R. and Y.A. Levendis, *On the deduction of single coal particle combustion temperature from three-color optical pyrometry.* Combustion and Flame, 2011. **158**(9): p. 1822-1836.
16. Hottel, H.C. and F.P. Broughton, *Determination of True Temperature and Total Radiation from Luminous Gas Flames.* Industrial & Engineering Chemistry Analytical Edition, 1932. **4**(2): p. 166-175.
17. Butler, B.W., M.K. Denison, and B.W. Webb, *Radiation heat transfer in a laboratory-scale, pulverized coal-fired reactor.* Experimental Thermal and Fluid Science, 1994. **9**(1): p. 69-79.

18. Smart, J., G. Lu, Y. Yan, and G. Riley, *Characterisation of an oxy-coal flame through digital imaging.* Combustion and Flame, 2010. **157**(6): p. 1132-1139.
19. Draper, T.S., D. Zeltner, D.R. Tree, Y. Xue, and R. Tsiava, *Two-dimensional flame temperature and emissivity measurements of pulverized oxy-coal flames.* Applied Energy, 2012. **95**: p. 38-44.
20. Clausen, S. and L.H. Sørensen, *Improved temperature measurements of burning char and coal particles using an FT-IR spectrometer.* Energy and Fuels, 1996. **10**(5): p. 1133-1141.
21. Rego-Barcena, S., R. Saari, R. Mani, S. El-Batroukh, and M.J. Thomson, *Real time, non-intrusive measurement of particle emissivity and gas temperature in coal-fired power plants.* Measurement Science and Technology, 2007. **18**(11): p. 3479-3488.
22. Bak, J. and S. Clausen, *FTIR emission spectroscopy methods and procedures for real time quantitative gas analysis in industrial environments.* Measurement Science and Technology, 2002. **13**(2): p. 150-156.
23. Yu, J. and M.C. Zhang, *Experimental and modeling study on char combustion.* Energy and Fuels, 2009. **23**(6): p. 2874-2885.
24. Yu, J., M.C. Zhang, G.F. Zhao, W.D. Fan, and Y.G. Zhou, *Temperature measurement for particle laden stream by FTIR emission/transmission spectroscopy.* Ranshao Kexue Yu Jishu/Journal of Combustion Science and Technology, 2003. **9**(5): p. 434-438.
25. Fletcher, T.H., J. Ma, J.R. Rigby, A.L. Brown, and B.W. Webb, *Soot in coal combustion systems.* Progress in Energy and Combustion Science, 1997. **23**(3): p. 283-301.
26. Draper, T., D. Zeltner, D.R. Tree, Y. Xue, C. Periasamy, T. Kang, and R. Tsiava, *Characterization of a primary-swirled, high oxygen participation coal flame: Flame temperature, emissivity, NO, and burnout measurements.* Proceedings of the Combustion Institute, 2013. **34**(2): p. 2779-2786.
27. Thornock, J., D. Tovar, D.R. Tree, Y. Xue, and R. Tsiava, *Radiative intensity, no emissions, and burnout for oxygen enriched biomass combustion.* Proceedings of the Combustion Institute, 2015. **35**(3): p. 2777-2784.
28. Tree, D.R. and J.A. Peart, *Two-color transmittance measurements in a pulverized coal reactor.* Proceedings of the Combustion Institute, 2000. **28**(2): p. 2361-2367.
29. Stimpson, C.K., A. Fry, T. Blanc, and D.R. Tree, *Line of sight soot volume fraction measurements in air- and oxy-coal flames.* Proceedings of the Combustion Institute, 2013. **34**(2): p. 2885-2893.
30. Seeker, W.R., G.S. Samuelsen, M.P. Heap, and J.D. Trolinger, *The thermal decomposition of pulverized coal particles.* Symposium (International) on Combustion, 1981. **18**(1): p. 1213-1226.
31. Andersson, K., R. Johansson, F. Johnsson, and B. Leckner, *Radiation Intensity of Propane-Fired Oxy-Fuel Flames: Implications for Soot Formation.* Energy & Fuels, 2008. **22**(3): p. 1535-1541.
32. Andersson, K., R. Johansson, S. Hjärtstam, F. Johnsson, and B. Leckner, *Radiation intensity of lignite-fired oxy-fuel flames.* Experimental Thermal and Fluid Science, 2008. **33**(1): p. 67-76.
33. Bäckström, D., R. Johansson, K. Andersson, F. Johnsson, S. Clausen, and A. Fateev, *Measurement and Modeling of Particle Radiation in Coal Flames.* Energy & Fuels, 2014. **28**(3): p. 2199-2210.
34. Butler, B.W. and B.W. Webb, *Local temperature and wall radiant heat flux measurements in an industrial scale coal fired boiler.* Fuel, 1991. **70**(12): p. 1457-1464.
35. Smart, J.P., P. O'Nions, and G.S. Riley, *Radiation and convective heat transfer, and burnout in oxy-coal combustion.* Fuel, 2010. **89**(9): p. 2468-2476.
36. Mehta †, R.S., M.F. Modest ‡, and D.C. Haworth, *Radiation characteristics and turbulence–radiation interactions in sooting turbulent jet flames.* Combustion Theory and Modelling, 2010. **14**(1): p. 105-124.
37. Marakis, J.G., C. Papapavlou, and E. Kakaras, *A parametric study of radiative heat transfer in pulverised coal furnaces.* International Journal of Heat and Mass Transfer, 2000. **43**(16): p. 2961-2971.

38. Ahluwalia, R.K. and K.H. Im, *Spectral radiative heat transfer in coal furnaces using a hybrid technique*, in *Other Information: PBD: [1994]*. 1994. p. Medium: ED; Size: 26 p.
39. Mengüc, M.P. and R. Viskanta, *A Sensitivity Analysis for Radiative Heat Transfer in a Pulverized Coal-Fired Furnace.* Combustion Science and Technology, 1987. **51**(1-3): p. 51-74.
40. Gorog, J.P., J.K. Brimacombe, and T.N. Adams, *Radiative heat transfer in rotary kilns.* Metallurgical Transactions B, 1981. **12**(1): p. 55-70.
41. Barr, P.V., J.K. Brimacombe, and A.P. Watkinson, *A heat-transfer model for the rotary kiln: Part II. Development of the cross-section model.* Metallurgical Transactions B, 1989. **20**(3): p. 403-419.
42. Boateng, A.A. and P.V. Barr, *A thermal model for the rotary kiln including heat transfer within the bed.* International Journal of Heat and Mass Transfer, 1996. **39**(10): p. 2131-2147.
43. Boateng, A.A., *7 - Freeboard Heat Transfer*, in *Rotary Kilns*, A.A. Boateng, Editor. 2008, Butterworth-Heinemann: Burlington. p. 173-203.
44. Andersson, K. and F. Johnsson, *Flame and radiation characteristics of gas-fired O2/CO2 combustion.* Fuel, 2007. **86**(5–6): p. 656-668.
45. Johansson, R., K. Andersson, and F. Johnsson, *The influence of particle and gaseous radiation in oxy-fuel combustion*, in *Clean Coal Conference*. 2011: Clearwater Florida.
46. Johansson, R., K. Andersson, and F. Johnsson, *Influence of ash particles on radiative heat transfer in air and oxy-fired conditions*, in *Clean Coal Conference,* . 2012: Clearwater Florida.
47. Johansson, R., B. Leckner, K. Andersson, and F. Johnsson, *Influence of particle and gas radiation in oxy-fuel combustion.* International Journal of Heat and Mass Transfer, 2013. **65**(0): p. 143-152.
48. Modest, M.F., *Chapter 11 - Radiative Properties of Particulate Media*, in *Radiative Heat Transfer (Second Edition)*. 2003, Academic Press: Burlington. p. 361-412.
49. Lighty, J.S., J.M. Veranth, and A.F. Sarofim, *Combustion Aerosols: Factors Governing Their Size and Composition and Implications to Human Health.* Journal of the Air & Waste Management Association, 2000. **50**(9): p. 1565-1618.
50. Kohse-Höinghaus, K., R.S. Barlow, M. Aldén, and J. Wolfrum, *Combustion at the focus: laser diagnostics and control.* Proceedings of the Combustion Institute, 2005. **30**(1): p. 89-123.
51. Radoux, F., T. Maalman, and N. Lallemant, *User manual Narrow Angle Radiometer Probe*, in *IFRF Doc No C73/y/10*. 1998: Ijmuiden, Netherlands.
52. Bäckström, D., D. Gall, M. Pushp, R. Johansson, K. Andersson, and J.B.C. Pettersson, *Particle composition and size distribution in coal flames – The influence on radiative heat transfer.* Experimental Thermal and Fluid Science, 2015. **64**(0): p. 70-80.
53. Smart, J.P., R. Patel, and G.S. Riley, *Oxy-fuel combustion of coal and biomass, the effect on radiative and convective heat transfer and burnout.* Combustion and Flame, 2010. **157**(12): p. 2230-2240.
54. Clausen, S., *Local measurement of gas temperature with an infrared fibre-optic probe.* Measurement Science and Technology, 1996. **7**(6): p. 888-896.
55. Heitor, M.V. and A.L.N. Moreira, *Thermocouples and sample probes for combustion studies.* Progress in Energy and Combustion Science, 1993. **19**(3): p. 259-278.
56. Michalski, L., K. Eckersdorf, and J. McGhee, *Temperature measurement*. Measuement science and technology. 1991: John Wiley & sons.
57. Cashdollar, K.L., *THREE-WAVELENGTH PYROMETER FOR MEASURING FLAME TEMPERATURES.* Applied Optics, 1979. **18**(15): p. 2595-2597.
58. Levendis, Y.A., K.R. Estrada, and H.C. Hottel, *Development of multicolor pyrometers to monitor the transient response of burning carbonaceous particles.* Review of Scientific Instruments, 1992. **63**(7): p. 3608-3622.
59. Tree, D.R., D.L. Black, J.R. Rigby, M.Q. McQuay, and B.W. Webb, *Experimental measurements in the BYU controlled profile reactor.* Progress in Energy and Combustion Science, 1998. **24**(5): p. 355-383.

60. Roy, S., J.R. Gord, and A.K. Patnaik, *Recent advances in coherent anti-Stokes Raman scattering spectroscopy: Fundamental developments and applications in reacting flows.* Progress in Energy and Combustion Science, 2010. **36**(2): p. 280-306.
61. Zhang, W., F. Johnsson, and B. Leckner, *Momentum probe and sampling probe for measurement of particle flow properties in CFB boilers.* Chemical Engineering Science, 1997. **52**(4): p. 497-509.
62. Knutson, E.O. and K.T. Whitby, *Aerosol classification by electric mobility: apparatus, theory, and applications.* Journal of Aerosol Science, 1975. **6**(6): p. 443-451.
63. Price, H.D., B. Stahlmecke, R. Arthur, H. Kaminski, J. Lindermann, E. Däuber, C. Asbach, T.A.J. Kuhlbusch, K.A. BéruBé, and T.P. Jones, *Comparison of instruments for particle number size distribution measurements in air quality monitoring.* Journal of Aerosol Science, 2014. **76**(0): p. 48-55.
64. Morris, W.J., D. Yu, and J.O.L. Wendt, *Soot, unburned carbon and ultrafine particle emissions from air- and oxy-coal flames.* Proceedings of the Combustion Institute, 2011. **33**(2): p. 3415-3421.
65. Black, D.L. and M.Q. McQuay, *Particle Characteristics in the Radiant Section of a Coal-fired Utility Boiler.* Combustion Science and Technology, 1998. **132**(1-6): p. 37-74.
66. Musculus, M.P.B. and L.M. Pickett, *Diagnostic considerations for optical laser-extinction measurements of soot in high-pressure transient combustion environments.* Combustion and Flame, 2005. **141**(4): p. 371-391.
67. Bengtsson, P.E. and M. Aldén, *Application of a pulsed laser for soot measurements in premixed flames.* Applied Physics B, 1989. **48**(2): p. 155-164.
68. Shaddix, C.R. and K.C. Smyth, *Laser-induced incandescence measurements of soot production in steady and flickering methane, propane, and ethylene diffusion flames.* Combustion and Flame, 1996. **107**(4): p. 418-452.
69. Axelsson, B., R. Collin, and P.E. Bengtsson, *Laser-induced incandescence for soot particle size and volume fraction measurements using on-line extinction calibration.* Applied Physics B, 2001. **72**(3): p. 367-372.
70. Mewes, B. and J.M. Seitzman, *Soot volume fraction and particle size measurements withlaser-induced incandescence.* Applied Optics, 1997. **36**(3): p. 709-717.
71. Axelsson, B., R. Collin, and P.-E. Bengtsson, *Laser-induced incandescence for soot particle size measurements in premixed flat flames.* Applied Optics, 2000. **39**(21): p. 3683-3690.
72. Lee, S.C. and C.L. Tien, *Optical constants of soot in hydrocarbon flames.* Symposium (International) on Combustion, 1981. **18**(1): p. 1159-1166.
73. Stull, V.R. and G.N. Plass, *Emissivity of Dispersed Carbon Particles.* Journal of the Optical Society of America, 1960. **50**(2): p. 121-125.
74. Dalzell, W.H. and A.F. Sarofim, *Optical Constants of Soot and Their Application to Heat-Flux Calculations.* Journal of Heat Transfer, 1969. **91**(1): p. 100-104.
75. Chang, H. and T.T. Charalampopoulos, *Determination of the Wavelength Dependence of Refractive Indices of Flame Soot.* Proceedings: Mathematical and Physical Sciences, 1990. **430**(1880): p. 577-591.
76. Foster, P.J. and C.R. Howarth, *Optical constants of carbons and coals in the infrared.* Carbon, 1968. **6**(5): p. 719-724,IN23,IN24,725-729.
77. Lohi, A., J.R. Wynnyckyj, and E. Rhodes, *Spectral measurement of the complex refractive index of fly ashes of canadian lignite and sub-bituminous coals.* The Canadian Journal of Chemical Engineering, 1992. **70**(4): p. 751-758.
78. Gupta, R.P. and T.F. Wall, *The optical properties of fly ash in coal fired furnaces.* Combustion and Flame, 1985. **61**(2): p. 145-151.
79. Goodwin, D.G. and M. Mitchner, *Flyash radiative properties and effects on radiative heat transfer in coal-fired systems.* International Journal of Heat and Mass Transfer, 1989. **32**(4): p. 627-638.
80. Patrick Arnott, W., H. Moosmüller, C. Fred Rogers, T. Jin, and R. Bruch, *Photoacoustic spectrometer for measuring light absorption by aerosol: instrument description.* Atmospheric Environment, 1999. **33**(17): p. 2845-2852.

81. Fleig, D., K. Andersson, F. Johnsson, and B. Leckner, *Conversion of sulfur during pulverized oxy-coal combustion.* Energy and Fuels, 2011. **25**(2): p. 647-655.
82. Kühnemuth, D., F. Normann, K. Andersson, F. Johnsson, and B. Leckner, *Reburning of nitric oxide in oxy-fuel firing-the influence of combustion conditions.* Energy and Fuels, 2011. **25**(2): p. 624-631.
83. Hjärtstam, S., R. Johansson, K. Andersson, and F. Johnsson, *Computational Fluid Dynamics Modeling of Oxy-Fuel Flames: The Role of Soot and Gas Radiation.* Energy & Fuels, 2012. **26**(5): p. 2786-2797.
84. Malkmus, W., *Random Lorentz Band Model with Exponential-Tailed S-1 Line-Intensity Distribution Function.* J. Opt. Soc. Am., 1967. **57**(3): p. 323-329.
85. Rivière, P. and A. Soufiani, *Updated band model parameters for H 2O, CO 2, CH 4 and CO radiation at high temperature.* International Journal of Heat and Mass Transfer, 2012. **55**(13-14): p. 3349-3358.
86. Stephen J, Y., *Nonisothermal band model theory.* Journal of Quantitative Spectroscopy and Radiative Transfer, 1977. **18**(1): p. 1-28.
87. Manickavasagam, S. and M.P. Menguc, *Effective optical properties of pulverized coal particles determined from FT-IR spectrometer experiments.* Energy & Fuels, 1993. **7**(6): p. 860-869.
88. Viskanta, R., A. Ungan, and M.P. Menguc, *Predictions of radiative properties of pulverized coal and fly-ash polydispersions.* Journal Name: Am. Soc. Mech. Eng., (Pap.); (United States); Journal Volume: 81-HT-24, 1981: p. Medium: X; Size: Pages: vp.
89. Lockwood, F.C. and N.G. Shah, *A new radiation solution method for incorporation in general combustion prediction procedures.* Symposium (International) on Combustion, 1981. **18**(1): p. 1405-1414.